

Packet Transmission Scheduling in Wireless Body Area Networks

by

Zhen Zhao

A Thesis submitted to the Faculty of Graduate Studies of

The University of Manitoba

in partial fulfillment of the requirements for the degree of

Master of Science

Department of Electrical and Computer Engineering

University of Manitoba

Winnipeg

May 2017

Copyright © 2017 by Zhen Zhao

Abstract

As the key component for ubiquitous realtime healthcare monitoring systems, wireless body area networks (WBANs) emerge as a promising solution to relieve the financial and social burdens resulting from the growth of aging population and rising healthcare costs. Although WBANs are commonly regarded as the extension of wireless sensor networks (WSNs), most existing studies on WSNs cannot satisfy the communication requirements because of complicated communication environments around the human body tissue and more stringent energy constraints in WBANs, which prompts a lot of research efforts recently. In this thesis, we focus on the packet transmission scheduling in WBANs, where we carefully study the energy efficient issue and investigate the channel shadowing effects. After presenting some fundamentals and related works, we propose a general analytical framework to evaluate the performance of IEEE 802.15.6 based CSMA/CA scheduling in WBANs, with joint considerations of instantaneous delay constraints and body shadowing effects. In addition, we also propose a multi-threshold based transmission strategy for joint data and energy scheduling in WBANs, where rechargeable sensors can efficiently manage their transmission energy allocations by simultaneously considering the amount of waiting packets in the buffers and available energy in the batteries. Extensive simulations are conducted to verify our proposed analytical models and demonstrate performance gains of our proposed strategy.

Acknowledgements

I would like to thank my supervisor, Prof. Jun Cai, for his continual support, encouragement and guidance throughout my master's study. Dr. Cai provided me with this precious studying opportunity at the University of Manitoba, gave me enough freedom on telecommunication research, led me to work on several software projects, and helped me to write my papers more logically. Besides, I really appreciate his suggestions about my world outlook on life and values, which will definitely be always guiding my life in the future. I am also sincerely grateful to Prof. Attahiru S. Alfa. for his excellent lectures and precious advice on queueing theories. In addition, I would like to thank my committee members, Prof. Pradeepa Yahampath and Prof. Nan Wu, for their insightful comments and helpful suggestions.

I am also grateful to my colleagues in the Network Intelligence and Innovation (NI²) Lab for all stimulating discussions in research. Particularly, I would express my sincere gratitude to Shiwei Huang and Changyan Yi for their kind guidance on telecommunication theories and valuable suggestions about paper researches and writings.

I thank my family for their boundless love and unconditional support. Thanks to my dear girlfriend, her patient accompanies helped me go through all the hardships during my master's study. This thesis cannot have been accomplished without their supports.

Contents

Abstract	ii
Acknowledgements	iii
List of Figures	vi
1 Introduction	1
1.1 Background and Motivations	1
1.2 Summary of Contributions	4
1.3 Outline of the Thesis	5
2 Fundamentals and Related Works	6
2.1 Overview of Wireless Body Area Networks	6
2.1.1 Network Characteristics	7
2.1.2 Architecture and Applications	9
2.1.3 Research Challenges	11
2.2 Packet Transmission Scheduling in Wireless Body Area Networks	13
3 An Analytical Framework for IEEE 802.15.6 Based Wireless Body Area Networks with Instantaneous Delay Constraints and Shadowing Interruptions	17
3.1 System Model	18
3.1.1 Network Framework	19
3.1.2 Wireless Channel Model	19
3.1.3 Medium Access Control	20
3.2 Formulation of the Queueing Model	24
3.2.1 Correlated Traffic Arrivals	25
3.2.2 Service Process with Shadowing Interruptions	25
3.2.3 Over-deadline Dropping Principle with Instantaneous Delay Constraints	27
3.3 Queueing Analysis	29
3.3.1 Buffer-overflowing Approximation	29
3.3.2 Matrix-Geometric Analysis	32
3.3.3 Stationary Distribution	36
3.3.4 Performance Metrics	38
3.4 Numerical and Simulation Results	41
3.4.1 Simulation Parameters	41
3.4.2 Queueing Dynamics Verification	42
3.4.3 Impacts of Body Shadowing Interruption	44

3.4.4	Impacts of Instantaneous Delay Constraint	45
4	Energy Efficient Packet Transmission Strategies for Wireless Body Area Networks with Rechargeable Sensors	48
4.1	System Model	49
4.1.1	Network Model	49
4.1.2	Channel Model	49
4.1.3	Queueing Model	50
4.2	Energy Efficient Transmission Strategy	51
4.3	Queueing Analysis	53
4.3.1	Stationary Analysis	53
4.3.2	Performance Measures	57
4.4	Energy Efficiency Optimization	58
4.5	Numerical Results	59
5	Conclusions and Future Works	63
5.1	Conclusion and Comments	63
5.2	Future Works	64
	References	66

List of Figures

2.1	An example of a WBAN in healthcare systems	7
2.2	The communication tiers in WBANs [1]	9
2.3	The applications of WBANs [2]	10
2.4	The power requirements and data rates in WBANs [3]	11
3.1	An illustration of the communication architecture in WBANs	18
3.2	The 2-tuple Absorbing Markov Chain at a medical sensor node	21
3.3	A new absorbing Markov Chain with a single absorbing state	24
3.4	The verification of packet waiting time distribution under different arrival intensities	43
3.5	The effect of shadowing interruption on the average waiting delay	44
3.6	The effect of shadowing interruption on the transmission failure probability	45
3.7	The effect of instantaneous delay limit on the average waiting delay	46
3.8	The effect of instantaneous delay limit on the transmission failure probability	47
4.1	Threshold-based queueing system under study	49
4.2	Energy efficiency comparison for different transmission strategies	60
4.3	Energy waste comparison for different transmission strategies	61
4.4	Packet dropping probability comparison for different transmission strategies	61
4.5	Average delay comparison for different transmission strategies	62

Chapter 1

Introduction

1.1 Background and Motivations

Advances in low-power wireless technologies, intelligent integrated circuits and low-cost miniaturized sensors have enabled a new generation of wireless sensor networks that could continuously detect vital physiological data profiling the human body activities, called wireless body area networks (WBANs) [4]. WBANs, also referred as body area networks (BANs) or as body sensor networks (BSNs), are a new type of network architecture that enables wireless data communication around the human body. WBANs have become a promising solution to relieve the financial and social burdens to meet increasing demands on ubiquitous realtime healthcare and fitness monitoring [5]. The inherently affordable and convenient features of WBANs can significantly improve the efficiency of healthcare services. Besides healthcare systems, WBANs can also supports a number of innovative and interesting applications such as sports, entertainments and military applications.

In WBANs, tiny and ultra-low-power sensors are deployed in, on or around the human body for continuously sensing vital physiological signals, such as electrocardiogram, heart rate, oxygen saturation, body temperature, blood pressure, etc. The sensed signals are then aggregated at a coordinator (or hub) via wireless links and forwarded to remote servers for interpretation and diagnosis. The coordinator can be a smart phone or any other smart

device, and ordinarily has less stringent constraints on processing and power capabilities compared with biosensors.

Although WBAN-based wireless technologies can provide advantages over the conventional monitoring systems, there are still many problems that prevent wide application of WBANs in practice [1]. Compared with traditional wireless sensor networks (WSNs), small lightweight sensors in WBANs have more strict energy constraints, especially in terms of transmit power. Besides, the sensor replacement or recharging, particularly for implanted sensors, may cause many discomforts for users with WBANs. More importantly, the radio frequency (RF) transmission, which is the only practical mechanism for data transmissions in WBANs [6], suffers considerably from human body shadowing in a highly variable way [7]. Furthermore, constrained by ultra-low power requirements, data transmissions in the vicinity of the human body become highly lossy and unreliable [8]. In addition, the entire WBAN is in motion due to postural body movements, so that the network topology changes with group-based movement rather than node-based movement. In that sense, WBANs are very similar to mobile ad hoc networks (MANETs) [9], but WBANs have more frequent topology changes.

All these problems bring new challenges on the packet transmission scheduling in WBANs, which has motivated a lot of research efforts in recent years. Compared with conventional scheduling schemes, WBANs bring two main research challenges: the complicated and unpredictable variation in channel conditions and more stringent energy-saving requirements. Specifically, affected by the human body shadowing, the wireless service in WBANs may be interrupted in a highly random way with respect to human bodies. Besides, small lightweight sensor devices in WBANs commonly have very scarce energy resources. Therefore, preserving energy at sensor nodes by design more efficient scheduling strategies becomes increasingly crucial to prolong the lifetime of WBANs. In addition, there are other unique challenges posed by WBAN applications, including low radio transmission range, private securities, severe mutual interference, and heterogeneous data collections from different sensors with different sampling rates.

The motivation of this thesis mainly concentrates on the following two aspects:

First, most existing works on energy-saving issues, such as sleep and wakeup strategies designs [10] and efficient routing protocol designs [11], were not feasible for WBANs due to the long-term continuous monitoring and low delay requirements. In WBANs, we should focus more on decreasing the amount of data that need to be transmitted as communication was ordinarily considered to be the most energy consuming operation [12]. Besides, since the communication environment around the human body is very complicated and body sensors are low-complexity devices that work in a very low power regime, the wireless service in WBANs may be interrupted in a highly variable way. However, such service interruption resulting from human body shadowing in WBANs has not been well addressed. Moreover, the arrival correlation which is one of most important features of telemedicine signals sensed from human bodies [13] was also ignored in the literature. To address these issues, in Chapter 3, we propose a novel energy-saving scheme with instantaneous delay constraints and design a random time limited single vacation to describe the shadowing interruptions.

Second, by considering the unreliable feature of communication links around the human body and the randomness of energy harvesting, the energy allocation should be adaptively adjusted based on the current status of the data buffer, energy battery and wireless channel. Therefore, in order to meet the stringent quality of service (QoS) requirements in WBANs, energy efficient transmission scheduling and energy allocation strategies are required. Although Markov decision process was widely adopted to formulate the joint data and energy scheduling problems, the high computational complexity made it infeasible for practical applications due to huge state spaces. In addition, most existing works on WBANs assumed independent and identically distributed (i.i.d.) fading channels, which ignored the channel correlation around the human body. In Chapter 4, we propose a multi-threshold based transmission strategy for joint data and energy scheduling in WBANs with the consideration of channel correlation.

In the following sections, we provide the brief summary of our contributions and then

conclude the chapter with the thesis organization.

1.2 Summary of Contributions

The contributions of this thesis are summarized as follows:

In Chapter 3, a general analytical framework is formulated to evaluate the performance of WBANs under the instantaneous delay constraints and body shadowing effects. Based on the IEEE standard, we construct a two-absorbing-state Markov chain to model the MAC protocol with error controls, and introduce a phase type (PH) distribution with a specific blocking rate to mathematically describe such a Markov chain. In the framework, body shadowing effects are considered as a shadowing interruption process, which is further modeled as a random time limited single vacation. We refer to the Markov arrival process to capture the correlations of arrival traffics in WBANs. In addition, we propose a novel energy-saving scheme to decrease packet transmissions, where the service of sensed packets is constrained by a firm instantaneous delay limit. The long-awaited packets with poor timeliness are considered to be valueless and will be dropped to guarantee the timeliness of valuable packets and avoid energy waste for transmitting valueless packets. Extensive simulations are conducted to validate the theoretical analysis and evaluate system performance. This work contributes to a journal paper, which is submitted to IEEE Transaction on Vehicular Technology.

In Chapter 4, we propose a multi-threshold based transmission strategy for joint data and energy scheduling in WBANs, where rechargeable sensors can efficiently manage their transmission energy allocations by simultaneously considering the amount of waiting packets in the buffers and available energy in the batteries. A queueing model is formulated to analyze the performance of the proposed transmission strategy. In our analysis, a discrete Markov arrival process (DMAP) is introduced to model the service process, which jointly considers channel correlations and energy allocations. Because of the existence of multiple thresholds in both data and energy buffers, a level dependent Quasi-Birth-and-

Death (QBD) Markov chain is developed for analyzing performance metrics in terms of the stationary queue length distribution, average delay, queueing throughput and average system-offline probability. At last, we formulate an optimization problem to find the optimal threshold settings and corresponding energy allocations for maximizing the energy efficiency while maintaining QoS requirements in terms of the average delay and system-offline probability. Simulation results are provided to verify our analytical models and demonstrate the performance gain of our proposed strategy in WBANs over counterparts. This work has contributed to an invited conference paper, which has been accepted by IEEE Vehicular Technology Conference (VTC'2017-Fall).

1.3 Outline of the Thesis

The rest of the thesis is organized as follows. Chapter 2 introduces some fundamentals and related works that are relevant to our research. In Chapter 3, we construct a general discrete time queueing system to model the operation of IEEE standard 802.15.6 CSMA/CA access mechanism integrating instantaneous delay constraints and shadowing interruptions. Motivated by threshold-based and state-aware scheduling strategies, a multi-threshold based strategy for joint data and energy scheduling is proposed and analyzed for WBANs with rechargeable sensors in Chapter 4. Finally, Chapter 5 concludes this thesis and summarizes some potential future extensions.

Chapter 2

Fundamentals and Related Works

In this chapter, fundamental knowledge and related literature are presented as the basis for future references. We first provide an overview of wireless body area networks including the network characteristics, communication architecture, potential applications, and research challenges. Although the packet transmission scheduling has been widely discussed in wireless communication networks, the traditional strategies were challenged by many new features in WBANs. Thus, we then provide a comprehensive literature review for most of recent researches on the packet transmission scheduling in WBANs.

2.1 Overview of Wireless Body Area Networks

With the growth of aging population [14] and the increasing demand for high quality of healthcare, existing medical systems and hospital facilities have been confronting a burden of overload. To overcome this issue, a new network concept, wireless body area networks (WBANs), has been proposed as a promising solution to revolutionize the telemedicine system, which adopts advanced information processing and communication technologies to enhance efficiency and flexibility of traditional medical services [15].

A WBAN typically consists of several sensors that collect various physiological changes of the human body, together with a central network coordinator (or called a hub).

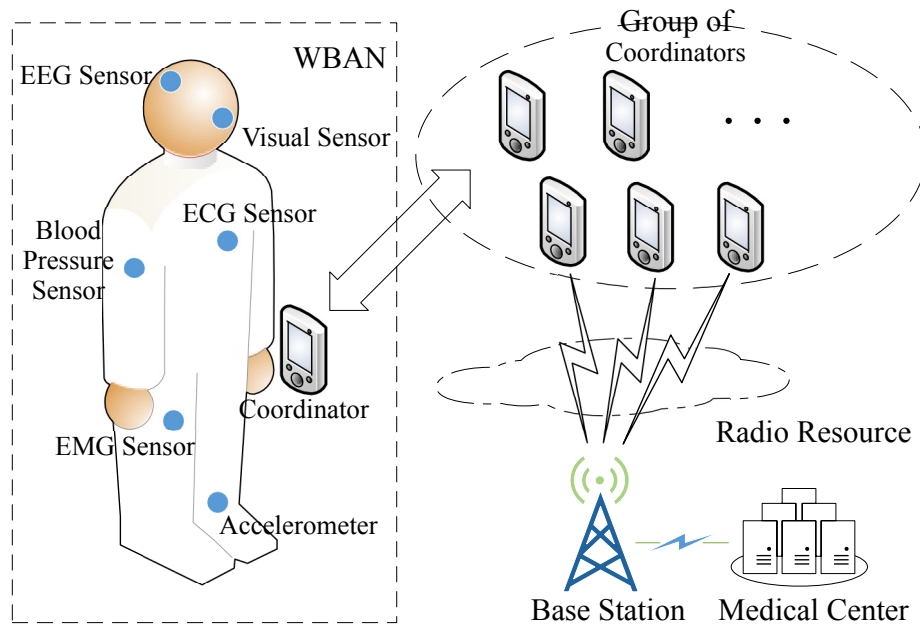


Figure 2.1: An example of a WBAN in healthcare systems

The sensors can be deployed around the human body, placed on the body surface, or even implanted inside the body to monitor the human body functions and the surrounding environment. The sensed signals are aggregated at the coordinator via wireless links and forwarded to remote servers for interpretation and diagnosis. An example of a WBAN in healthcare systems is illustrated in Fig. 2.1. WBANs have the potential to facilitate inexpensive and continuous health monitoring, computer-assisted rehabilitation, and early detection of medical conditions, with real-time record updates through the Internet.

2.1.1 Network Characteristics

WBANs is commonly considered to be the extension of wireless sensor networks (WSNs). However, compared with conventional WSNs, WBANs have their own special characteristics and requirements, which distinguish them from general WSNs and also introduce new technical challenges. Formally, the main characteristics are summarized as follows [16]:

- **Node Deployment and Density:** WBAN sensors are deployed in, on or around the

human body and typically form a star-topology network together with a powerful coordinator, where the wireless communication is centrally organized [17]. Besides, affected by human motions, the data transmission in WBANs is comparatively sensitive and unreliable. WSNs commonly need to add redundant nodes to solve the node lost or failure problem which is unnecessary in WBANs, and thus WBANs do not have high node density. In addition, WBAN sensors are often very heterogeneous and may have very different demands in terms of data rates and reliability [18].

- **Limited Energy:** WBANs commonly need to support continuous monitoring for months or even years, but biosensors comprising WBANs have very limited energy resources available due to the small form factor [19]. Moreover, the sensor replacement and recharging, especially for implanted sensors, are very difficult and sometimes invasive to human bodies. Signal transmission attenuation is very large because of the specificity of the body tissue structure and the shadowing effect [16]. Thus, WBAN biosensors must be extremely frugal in their energy managements.
- **Reliability:** The reliability of WBANs relies on the transmission delay and packet dropping probability. Different from the requirements in traditional WSNs, whose design objective is commonly to maximize network throughput (or minimize the packet dropping probability), WBANs draw more attention on whether the data can be timely transmitted to the medical center, i.e., a lower transmission delay. Moreover, an extremely low transmit power for biosensors is adopted to minimize the interference and cope with health concerns [20]. Since the delay is directly affected by the channel stability and energy allocations, the high randomness of wireless channel in the proximity of human bodies and the low transmission power usually greatly increase the transmission delay.
- **Mobility and Security:** Since wearers of WBANs may move around, WBAN nodes affiliated with the same wearer may move together and in the same direction [21]. In contrast, WSN nodes are usually thought of as stationary, and any node mobility

does not occur in groups. Besides, in WBANs, stringent security mechanisms are also required to keep the user data, especially the medical data, strictly private, confidential and safe.

2.1.2 Architecture and Applications

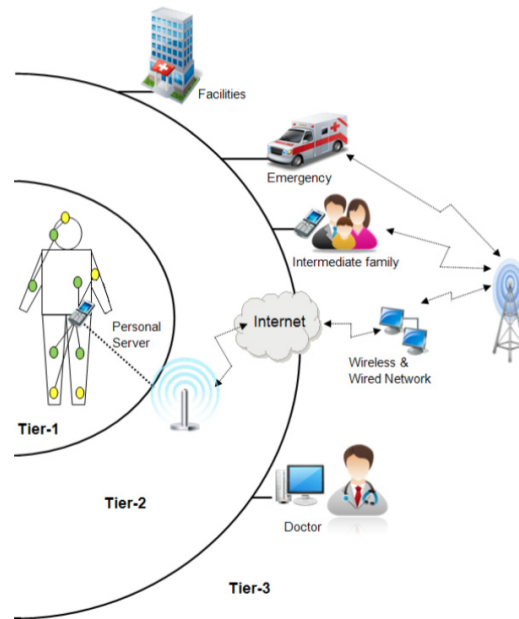


Figure 2.2: The communication tiers in WBANs [1]

As shown in Fig.2.2, the generalized system architecture of a WBAN can be divided in three fundamental communication levels or tiers [1, 22, 23].

- Tier-1 communication (intra-WBAN). The intra-WBAN communication refers to the radio communication range of about 2 meters around the human body [23]. In the intra-WBAN, various biosensors transmit collected body signals to a personal server (PS) (works as a coordinator or hub) which in turn forwards the processed physiological data to an access point (AP) in Tier-2.
- Tier-2 communication (inter-WBAN). Inter-WBANs usually involve the communication between the PS and one or more APs, and aim at interconnecting WBANs with other networks, such as cellular networks, WLAN or even other WBANs.

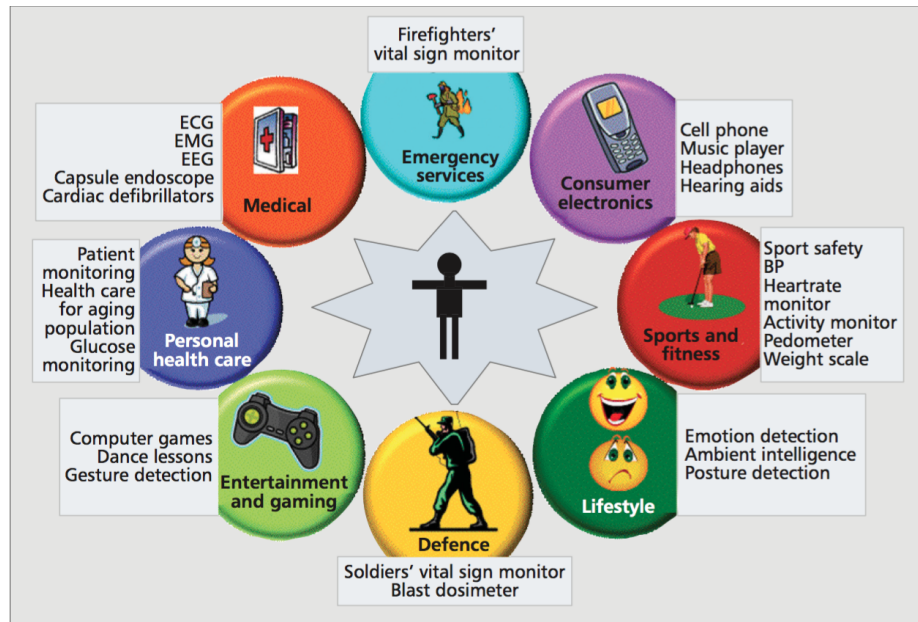


Figure 2.3: The applications of WBANs [2]

- Tier-3 communication (beyond-WBAN). The beyond-WBAN communication is designed for metropolitan areas and is usually application-specific [1]. This tier involves communication between a WBAN and an outside network, e.g., internet or some medical centers [22].

WBAN is an emerging enabling technology with a broad range of potential applications and use cases in diverse application domains including medical, fitness and wellness management, military, sport, entertainment and so on. Based on the IEEE standard 802.15.6 [24], the WBANs application can be divided into medical and non-medical applications. The use of WBANs for medical applications is expected to enable more effective management and detection of illnesses and reaction to crisis [25]. In such applications, WBANs continuously collect vital information of patients and forward it to a remote monitoring station for real-time analysis [26]. Non-medical applications commonly include five subcategories, real-time streaming, entertainment, emergency (non-medical) applications, emotion detection and secure authentications [1]. Fig. 2.3 illustrates all the potential WBANs applications.

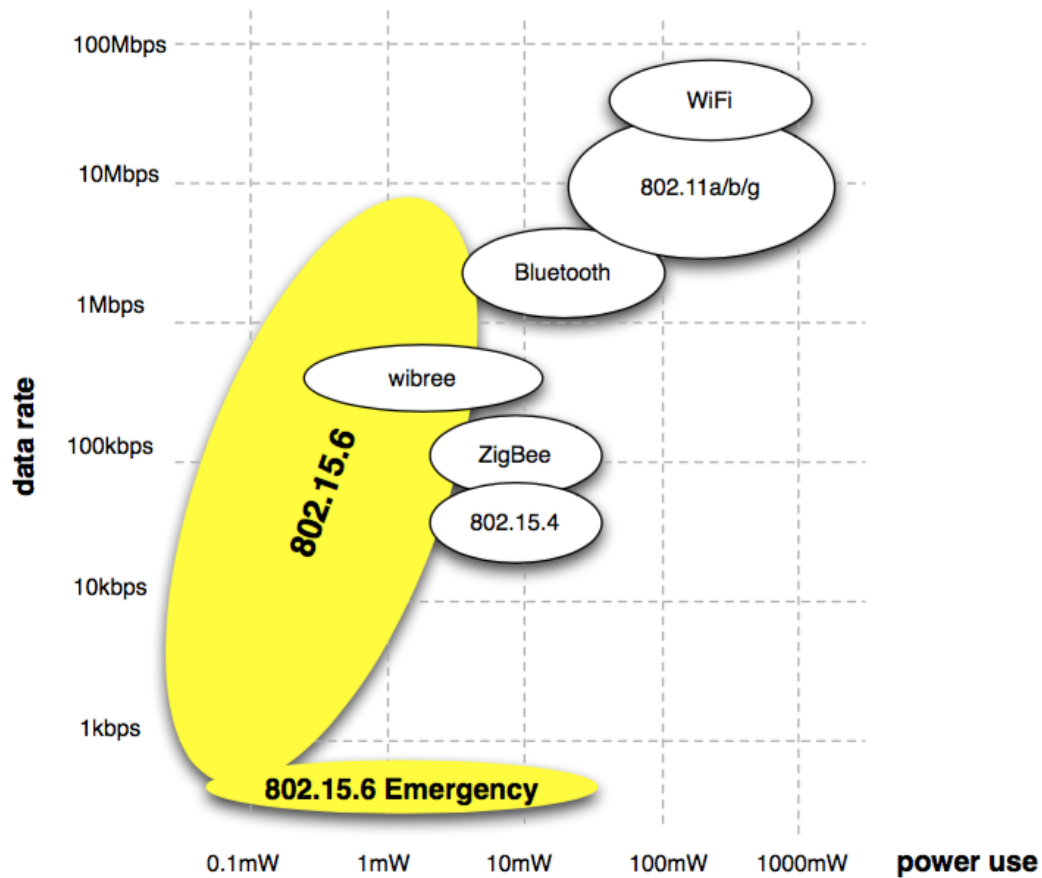


Figure 2.4: The power requirements and data rates in WBANs [3]

2.1.3 Research Challenges

Despite the suitability of IEEE 802.15.6 for WBANs [24], successful systems are highly dependent on the characteristics of the wireless channel around human bodies and specific application requirements, which are still confronted with lots of challenges. In this section, we list some major research challenges that need to be taken into consideration in the design of WBANs.

- Extreme energy efficiency: In order to deliver the levels of comfort and unobtrusiveness required for widespread adoption, WBAN biosensors must be small [27]. However, the size requirement obviously limits the size of the batteries and further the energy storage. In addition, depending on the specific applications, WBANs are commonly required to work unobtrusively for months or even years. Therefore,

achieving a high energy efficiency is the most important goal in WBANs.

- **Unique characteristics of the wireless channel:** The behavior of the wireless channel around the human body poses a unique set of challenges to reliable communications. It has been widely recognized that the wireless propagation environment in the vicinity of the human body is considerably different from conventional network environments [28]. The radio frequency (RF) transmission, which is the only practical mechanism for data transmission in WBANs [6], suffers significantly from human body shadowing in a highly variable way with respect to human bodies [7] [8]. Human motions can constantly change the attenuation at a rate that depends on the type of physical activity. Furthermore, constrained by ultra low power requirements, the data transmission around the human body becomes very unreliable and is very sensitive to human motions.
- **Interference management:** Biosensors in WBANs can be centrally coordinated by the hub, thus allowing a large number of devices to coexist in a single network without interference with each other. However, the coordination may become very complicated when multiple people wearing WBANs come into the range of each other since closely-located WBANs will cause severe mutual interference. This issue becomes even more crucial in the high coverage areas [29], such as hospitals or nursing homes. Besides, the human motions are unpredictable from a network's viewpoint, which may lead to networks randomly moving into and out of range of each other. Therefore, efficient interference mitigation schemes are required to manage the inter-WBANs interference [30].
- **Heterogeneous requirements:** In order to accommodate higher throughput applications, WBANs need to support a wide range of data rates varying from 1 Kbit/s to 10 Mbit/s [24], while still satisfying the high reliability and low-latency required in many WBAN applications. Since biosensors deployed around human bodies commonly aim at monitoring different physiological signs, they usually have

different demands in terms of data rates and reliability. Furthermore, as shown in Fig. 2.4, the existing technologies like Bluetooth or Zig-Bee cannot simultaneously meet the data and power requirements for all WBAN applications.

- **Security and Privacy:** Since the collected data in WBANs has significantly legal, financial and private meanings, keeping the information private, confidential and authorized is a fundamental requirement. However, the conventional security and private mechanisms are not feasible for WBANs due to stringent resource constraints in terms of energy, memory, processing ability, as well as the lack of user interface, unskilled users, and global roaming [2]. As a high priority for safe communications, security issues should be well addressed in WBANs [31].

2.2 Packet Transmission Scheduling in Wireless Body Area Networks

The traditional packet transmission scheduling strategies were challenged by many new features in WBANs. In this section, we present a general survey for most of recent researches on transmission scheduling in WBANs. To facilitate reading, we classify the existing researches in three groups in terms of energy efficient medium access control (MAC) protocol designs, transmission scheduling with energy harvesting, and IEEE standard based analyses and improvements.

1) Energy Efficient MAC Protocol Designs: In WBANs, energy limitation plays a dominant role in determining average system performance and lifetime [32]. The unique channel characteristics, coupled with the need for extreme energy efficiency in healthcare applications, require novel solutions in MAC protocols. Generally, MAC protocols for WBANs can be categorized into two types: contention-based and schedule-based. In contention-based protocols, such as CSMA/CA, sensors have to compete to gain the transmission opportunity. Such protocols have no need to establish infrastructure and

have shown good scalability, so that they may be affected less by human motions. But contentions among sensor nodes may incur packet collisions and further cause great energy wastage. On the other hand, schedule-based protocols, such as TDMA, divide the channel into time slots and explicitly allocate slots to nodes. Each node transmits data in their own slots and keeps asleep in other slots. Consequently, collisions are avoided and energy waste is reduced. However, the performance of TDMA-based designs is deteriorated due to the large overhead necessitated by the synchronization, and it will inevitably introduce extra delay and energy consumption.

To overcome these weaknesses, there have been a lot of researches working on the medium access control (MAC) protocol design with emphases on energy efficiency [33,34]. Omeni et al. in [35] proposed a TDMA-based MAC protocol to reduce the collision and energy cost, which was based on centrally controlled wakeup and sleep mechanisms to maximize energy efficiency. In [36], an energy efficient MAC protocol using modified TDMA structure with extra reserved slots was proposed, where the reserved slots were used for re-transmission based on sensors' requests. Li et al. in [13] proposed a TDMA-based MAC protocol with a novel synchronization scheme, where heartbeat rhythm information extracted from the sensory data was exploited to synchronize the sensors. In [37], a contention-based MAC protocol designed for falls assessment was presented to guarantee different prioritized data latency requirements. In the design, high priority nodes could interrupt low priority nodes and exploit data fusion to improve system throughput. Su et al. in [38] proposed a battery-aware TDMA based MAC protocol with cross-layer design to maximize the network lifetime. In summary, the main goal of these works was to make full use of limited energy to transmit more sensed packets under average delay and packet dropping constraints, i.e., to achieve a higher system throughput with average QoS provisioning. However, average requirements are not sufficient to guarantee system performances in practice, especially when long-tail traffic occurs [39] [40], i.e., waiting delays need to be constrained in an instantaneous sense instead of in the average sense.

In conventional WSNs, sleep and wakeup strategies [10] were widely adopted to reduce

the energy waste and prolong the system lifetime. However, these strategies are not feasible for WBANs, which need to satisfy long-term continuous monitoring and low delay requirements. In WSNs, energy can also be significantly saved through improving routing protocols [11]. However, this method is still not applicable for WBANs because body sensors are commonly very proximate, leading to a single-hop topology [41]. Different from conventional WSNs, energy-saving techniques in WBANs frequently focused on decreasing the amount of data that need to be transmitted [12] since communication was ordinarily considered to be the most energy consuming operation for sensors [42]. For that purpose, IEEE standard 802.15.6 [24] specified re-transmission limits and Ghasemzadeh et al. in [41] investigated the communication minimization by means of buffers in WBANs. However, waiting delays of packets have not been considered in these works. Since packets that have been waiting for a long time are considered to be less valuable due to their poor timeliness [43], it is unnecessary to transmit these valueless packets, so as to save the transmission energy.

2) *Transmission Scheduling with Energy Harvesting*: Since energy harvesting is projected to be an ideal solution for eliminating the stringent energy constraints, the research interests in transmission scheduling with energy harvesting have significantly increased [44]. In WBANs, the human body is surrounded by various energy sources, such as solar, wind, human motion, radio frequency, and body heat, which make energy harvesting become a promising solution to relieve energy burdens. Affected by the randomness of energy harvesting, energy efficient transmission scheduling and energy allocation strategies are required to meet stringent quality of service requirements in WBANs [45]. Markov decision process (MDP) [46] was widely adopted to formulate such joint data and energy scheduling problems [47], [48]. However, the high computational complexity made it infeasible for practical applications with multiple queues and huge state spaces. Xiao et al. in [49] defined several transmission power levels and adapted transmit power in real-time based on feedback information from the receiver. Su and Zhang in [38] introduced two thresholds to control data transmissions based on data queue dynamics.

Chiti et al. in [50] proposed a novel cross-layer protocol that utilized a battery threshold to switch sensor working modes. However, more general multi-threshold cases with joint considerations of battery states and packet queuing characteristics are not studied in these works. In addition, most existing works on WBANs assumed independent and identically distributed (i.i.d.) fading channels for simplicity and tractability [51]. However, since wireless links around human bodies are closely related to human motions that usually follow a stable moving pattern, the channel correlation around the human body [52] cannot be ignored.

3) *IEEE Standard based Analyses and Improvements:* With the aid of the scientific and industrial communities, the IEEE Task Group 6 published the IEEE 802.15.6 standard for WBANs on February, 29 2012 [24]. The standard defined a new set of PHY layer and MAC layer specifications for short-range wireless communications in the vicinity of, or inside the human body. More specifically, it presented supports for heterogeneous QoS, extremely low power and high data rates, defined specific priorities for different kinds of traffics, and designed a contention window updating mechanism with re-transmission limits for access control. These new features motivated a lot of researches on performance evaluation for IEEE standard 802.15.6 based WBANs [53–56]. Rashwand et al. in [53] and [54] presented a Markov chain-based analysis under both non-saturation and saturation traffic conditions. Ullah et al. [55] provided a non-Markovian analysis in terms of throughput and average delay limits. In [56], a discrete-time Markov chain was constructed to model the IEEE 802.15.6 CSMA/CA access protocol with an immediate acknowledge (I-ACK) policy under non-ideal channel conditions. However, all these works ignored the arrival correlation that is one of most important features of telemedicine signals sensed from human bodies [13]. Moreover, the unreliability of RF communication around the human body, especially the body shadowing effect, has not been well modeled in these works.

Chapter 3

An Analytical Framework for IEEE

802.15.6 Based Wireless Body Area

Networks with Instantaneous Delay

Constraints and Shadowing

Interruptions

In this chapter, a novel queueing analytical framework is proposed to evaluate the performance of IEEE 802.15.6-based CSMA/CA scheduling in wireless body area networks with joint consideration of instantaneous delay constraints and body shadowing effects. Specifically, we develop an absorbing Markov chain to model the IEEE standard defined medium access process with error controls, and design a random time limited single vacation to describe the potential body shadowing interruption process. To guarantee the timeliness of received packets and avoid energy waste for transmitting valueless packets, an instantaneous delay constraint is carefully considered, which then is characterized by an over-deadline packet dropping process with a predefined waiting deadline. In our analysis, a Markovian arrival process is also adopted to capture the correlation of arrival traffic,

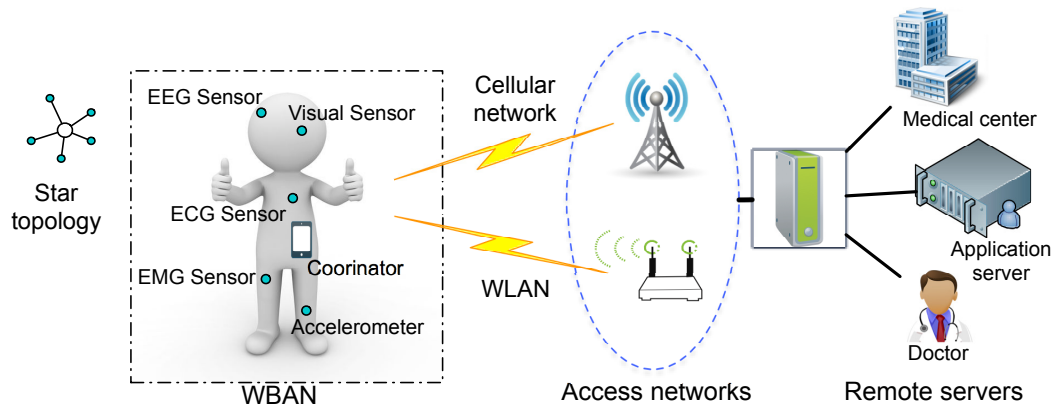


Figure 3.1: An illustration of the communication architecture in WBANs

and all other random processes are modeled by phase type distributions, which make our framework more general and comprehensive. To address the inherent complexity of the original model, based on the transient queueing analysis, we develop a buffer-overflowing queueing principle to approximate the over-deadline packet dropping principle by solving a buffer length optimization problem. After that, we construct a multidimensional discrete-time Markov chain to analyze the stationary distribution through the matrix-geometric method. Performance metrics, such as the average delay, waiting time distribution, and packet transmission failure probability are derived. The accuracy of our proposed analytical framework is validated by extensive simulations. Based on the result analysis, we justify the importance of instantaneous delay limits comparing with mean constraints, and investigate the impact of human body shadowing on system performance.

3.1 System Model

In this section, we describe the system model under consideration by introducing the communication architecture of WBANs, wireless channel model and IEEE 802.15.6 based MAC protocol.

3.1.1 Network Framework

We concentrate on a continuous healthcare monitoring system where one person is equipped with a WBAN. The general architecture is based on the standard IEEE 802.15.6 [24], as shown in Fig. 3.1. In particular, we mainly focus on the up-link transmissions in intra-WBAN (communications from sensors to the coordinator). N various medical sensors are deployed on the human body, and a powerful personal device, such as a smart phone, works as a coordinator. Usually, these nodes form a star-topology network and low-power sensors transmit the sensed physiological signals to the coordinator with a constant power through one-hop communication [38].

The time axis is divided into slots with equal lengths. Each data packet requires at least one time slot for its transmission and there is at most one new packet arrival within a time slot. We assume that all the events that occur during a time slot are observable at the end of the slot. Furthermore, we also assume that all packet arrivals occur just before the end of a slot and services terminate at the end of a slot, i.e., *late arrival with delayed access* [57].

3.1.2 Wireless Channel Model

Different from the conventional wireless networks, the distance is no longer a dominant factor that affects the signal attenuation in WBANs. Instead, small-scale fading has more influences on transmitted signals due to the complex structure of the body shape and human tissue [58]. Ordinarily, the wireless link in WBANs can be characterized by a slow flat fading channel [38]. Since the line of sight path is much stronger than others, the channel state, characterized by the received signal-to-noise ratio (SNR), follows an independent and identically distributed (i.i.d.) Rician-square (the envelop follows a Rician distribution) distribution among time slots but remains unchanged within each time slot [59]. The probability density function (PDF) of the received SNR (γ) is given by

$$\rho(\gamma) = \frac{\kappa + 1}{\bar{\gamma}} \exp\left[-\frac{\gamma(\kappa + 1)}{\bar{\gamma}} - \kappa\right] I_0\left(2\sqrt{\frac{\gamma\kappa(\kappa + 1)}{\bar{\gamma}}}\right), \quad (3.1)$$

where $I_0(\cdot)$ is the modified Bessel function of the first kind and 0th order. κ and $\bar{\gamma}$ denote the Rician K-factor (i.e., secular-to-scattered power ratio) and average SNR, respectively. Furthermore, by adopting the non-coherent differential encoded binary phase shift keying (DPSK) modulation scheme in WBANs [60], the average bit error rate (BER) under the Rician fading channel is

$$\bar{P}_e^b = \int P_e^b(\gamma)\rho(\gamma)d\gamma = \frac{1 + \kappa}{2(1 + \bar{\gamma} + \kappa)} \exp\left(-\frac{\kappa\bar{\gamma}}{1 + \bar{\gamma} + \kappa}\right), \quad (3.2)$$

where $P_e^b(\gamma)$ is the probability of BER in AWGN channel at a specific value of SNR γ . Therefore, the average packet error rate \bar{P}_e for a M -bit packet equals

$$\bar{P}_e = 1 - (1 - \bar{P}_e^b)^M. \quad (3.3)$$

3.1.3 Medium Access Control

According to the IEEE 802.15.6 stand, the medium access control (MAC) protocol for intra-WBAN consists of the slotted carrier sense multiple access with collision avoidance (CSMA/CA) [24] and automatic repeat request (ARQ) mechanism for error recovery. The standard specified eight user-priorities (UP) with different values of the minimum and maximum sizes of contention windows based on different traffic designations, and also a special contention window updating mechanism. Specifically, the contention window $W_{i,r}$ at a node i is represented as

$$W_{i,r} = \begin{cases} CW_{i,min} & \text{if } r = 0 \\ W_{i,r-1} & \text{if } r \text{ is an odd number, and } 1 \leq r \leq R \\ \min\{2W_{i,r-1}, CW_{i,max}\} & \text{if } r \text{ is an even number, and } 2 \leq r \leq R \end{cases}, \quad (3.4)$$

where r denotes the number of re-transmissions that a data packet has underwent, and R is the transmission retry limit. $CW_{i,min}$ and $CW_{i,max}$ represent the minimum and maximum contention windows of node i respectively, and depend on the traffic priority of node i . With this contention-based MAC, the probability that the channel is accessed by node i can

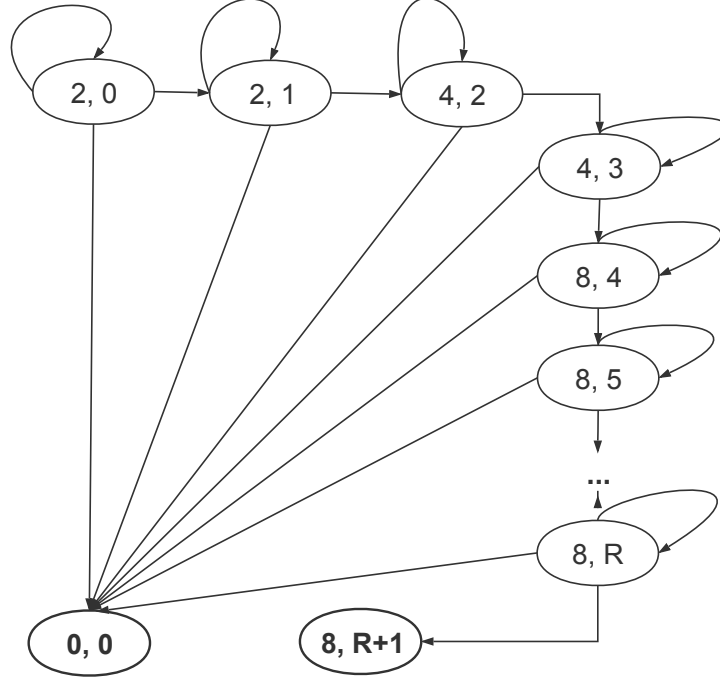


Figure 3.2: The 2-tuple Absorbing Markov Chain at a medical sensor node

be calculated as [61]

$$Pa(W_{i,r}) = \sum_{j=1}^{W_{i,r}} \left[\frac{1}{W_{i,r}} \prod_{k=1, k \neq i}^N \left(\frac{W_k - j}{W_k} \right) \right]. \quad (3.5)$$

Note that the channel is occupied by the node i for its packet transmission until the packet is successfully transmitted or blocked after R re-transmissions.

Furthermore, we formulate the service process for the node i as a two-tuple $(W_{i,r}, r)$ discrete time absorbing Markov chain, where $(0, 0)$ and $(CW_{i,max}, R+1)$ are two absorbing states, representing the service process is terminated due to the successful transmission and failed transmission after R retries, respectively. One example of such a Markov chain for a medical sensor node ($CW_{min} = 2, CW_{max} = 8$) is illustrated in Fig. 3.2. Then the transition probabilities of the formulated 2-tuple Markov chain at node i could be calculated

as follows. For the transitions between two transient states ($0 < r < R + 1$), we have

$$P1(r) = P_{rob}\{(W_{i,r}, r)|(W_{i,r}, r)\} = 1 - Pa(W_{i,r}), \quad (3.6)$$

$$P2(r) = P_{rob}\{(W_{i,r+1}, r + 1)|(W_{i,r}, r)\} = \bar{P}_e Pa(W_{i,r}), \quad (3.7)$$

where $P1(r)$ represents the situation that the service remained in the same state since the sensor failed accessing the channel, and $P2(r)$ represents the situation that the service switched to the next adjacent state when the channel was successfully accessed but transmission errors happened. Similarly, for the transition probabilities from any transient state to the absorbing state, we have

$$P0(r) = P_{rob}\{(0, 0)|(W_{i,r}, r)\} = \begin{cases} (1 - \bar{P}_e)Pa(W_{i,r}) & \text{if } 0 \leq r \leq R \\ 0 & \text{if } r = R + 1 \end{cases}, \quad (3.8)$$

$$P3(r) = P_{rob}\{(CW_{i,max}, R + 1)|(W_{i,r}, r)\} = \begin{cases} 0 & \text{if } 0 \leq r < R \\ \bar{P}_e Pa(W_{i,R}) & \text{if } r = R \end{cases}. \quad (3.9)$$

Note that for $P0(r)$, only when the sensor successfully gained the channel access opportunity and no transmission errors occurred, the packet can be successfully served, i.e., absorbed in state $(0, 0)$. $P3(r)$ represents the case that packet re-transmissions exceeded the retry limit R , which occurred only when a packet had been re-transmitted R times before the past slot, and the sensor successfully accessed the channel but failed transmitting the packet in the past slot because of errors. In summary, the transition probability matrix \mathbf{P}_t of the formulated 2-tuple absorbing Markov chain can be represented as

$$\mathbf{P}_t = \begin{bmatrix} Q & H \\ 0 & I_2 \end{bmatrix},$$

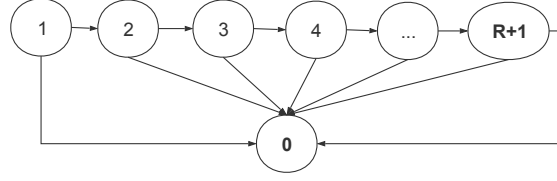


Figure 3.3: A new absorbing Markov Chain with a single absorbing state

under service is blocked due to reaching the re-transmission limit at the absorbing state $(CW_{i,max}, R + 1)$. Define ρ_d as the blocking rate of all these 'served' packets. Then ρ_d can be calculated as

$$\rho_d = \frac{b_{(CW_{i,max}, R+1)}}{b_{(0,0)} + b_{(CW_{i,max}, R+1)}}. \quad (3.14)$$

To simplify the structure of the two-tuple Markov chain, we introduce a new Markov chain with a single compound absorbing state, as shown in Fig.3.3. Let $K \in \{0, 1, 2, \dots, R, R+1\}$ denotes the compound state of $(W_{i,r}, r)$ in the new Markov chain. Then, $K = 0$ represents the absorbing state with blocking rate ρ_d , while $K \neq 0$ represents the transient state corresponding to the state $(W_{i,K-1}, K - 1)$ in the 2-tuple Markov chain. This newly introduced absorbing Markov chain can be represented by a phase type distribution (β, S) of order $n_s = R + 1$, and the associated transition probability matrix is given by

$$\mathbf{P}'_t = \begin{bmatrix} 1 & 0 \\ \mathbf{s} & S \end{bmatrix},$$

where $S = \mathcal{Q}$, $\mathbf{s} = \mathbf{1} - S\mathbf{1}$. Similar to the two-tuple Markov chain, the initial probability vector β is given by, $\beta = [\beta_1, \beta_2, \dots, \beta_R, \beta_{R+1}] = [1, 0, \dots, 0]$ and $\beta_0 = 1 - \beta\mathbf{1} = 0$.

3.2 Formulation of the Queuing Model

In this section, the IEEE 802.15.6-based CSMA/CA scheduling at a single sensor is modeled as a discrete time queuing system with random time limited vacations. Since various different types of biosensors are independent from each other in WBANs, we only focus on one general sensor node and similar analysis can be performed on any other type

of sensors. The basic queueing components (arrival process, service process, and service principle) are described as follows.

3.2.1 Correlated Traffic Arrivals

Since the packet inter-arrival time is usually correlated in WBANs [13], we model the packet arrival process at a sensor node as a Markovian arrival process (MAP), which has been widely used to fit different arrival patterns with highly correlated inter-arrival times [62]. The formulated MAP is associated with an absorbing Markov chain and the packet arrival probability at any time slot depends on both current and previous states (phases). Besides, the MAP can be described by two sub-stochastic matrices D_0 and D_1 of dimension n_a , where the elements $(D_0)_{ij}$ and $(D_1)_{ij}$ represent the transition probabilities from state i to state j without and with a packet arrival, respectively. Let $D = D_0 + D_1$. Then the matrix D is stochastic and irreducible, and $D\mathbf{1} = \mathbf{1}$, where $\mathbf{1}$ represents a column vector of ones with an appropriate dimension. Given D_0 and D_1 , the autocorrelation between inter-arrival times can be captured as [62]

$$Pr\{X_i = k\} = \pi D_0^{k-1} D_1 \mathbf{1}, \quad k \geq 1, \quad (3.15)$$

where X_i represents the i th inter-arrival time, $\pi = \pi(I - D_0)^{-1} D_1$, and $\pi\mathbf{1} = 1$.

3.2.2 Service Process with Shadowing Interruptions

Different from conventional communication environments, the data transmission between sensor nodes and the coordinator is very complicated in WBANs. This is because the human body has a complex shape and people are usually in motion, which result in highly random changes in the relative locations between sensors and the coordinator. Therefore, the strength of a received signal in WBANs is greatly affected by the physical location and orientation of the nodes in relation to each other as well as the human body [58]. Moreover, since WBANs are deployed around human bodies and have to be user-harmless,

the transmission power is required to stay at a very low level. Consequently, the packet transmission is more likely to be interrupted when the wireless link is blocked by the human body. In this chapter, we model the human body shadowing effect on the wireless service as a shadowing interruption process. However, mathematically modeling such a shadowing interruption process is very difficult due to the following challenges

- The wireless link for data transmissions could be blocked by the human body shadowing at any time. Therefore, the working or effective duration T_1 of a wireless link is a random variable with a general distribution.
- Similarly, a blocked wireless link may rebecome effective at any time. i.e., the interruption period for a wireless link, denoted by T_2 , is also a generally distributed random variable.

To address these issues, we introduce two general PH distributions to describe the randomness of T_1 and T_2 , which are denoted as (α, T) with order n_b and (ϕ, V) with order n_v , respectively. The selection of PH distribution is because it can approximately model any arbitrary distribution through moment matching approach based on three moments [63].

Consequently, a packet in the queue can be correctly received at the coordinator only if the link is unblocked by the human body and the packet service is successful. As for the human body blocking effect, which has been described by a shadowing interruption process, we model it as a interruption vacation with random time limited visits. Specifically, the server will be available for a random amount of time slots, T_1 , and will be blocked to go on an interruption vacation with a random time duration, T_2 . Thus, the probability $P_f(k_1)$ that the server attends to the queue for k_1 time slots (i.e. $T_1 = k_1$), and the probability $P_v(k_2)$ that the server takes k_2 time slots to return from an interruption vacation (i.e. $T_2 = k_2$) can be calculated as

$$P_f(k_1) = \begin{cases} \alpha_0 & k_1 = 0 \\ \alpha T^{k_1-1} \mathbf{t} & k_1 \neq 0 \end{cases}, \quad (3.16)$$

$$P_v(k_2) = \begin{cases} \phi_0, & k_2 = 0 \\ \phi V^{k_2-1} \mathbf{v} & k_2 \neq 0 \end{cases}, \quad (3.17)$$

where $\mathbf{t} = \mathbf{1} - T\mathbf{1}$ and $\mathbf{v} = \mathbf{1} - V\mathbf{1}$.

Recall that the packet service process, which is determined by the MAC protocol and the corresponding controlling schemes (e.g. error controls), has been modeled by a PH distribution (β, S) of order $R + 1$ with a blocking rate ρ_d in Section 3.1.3. The mean service rate μ can be derived as $\mu^{-1} = \beta(I - S)^{-1} \mathbf{s}$. Hence when server is on the working state, the probability $P_s(t)$ that a packet was served by using t time slots can be represented as

$$P_s(t) = \begin{cases} \beta_0 & t = 0 \\ \beta S^{t-1} \mathbf{s} & t \neq 0 \end{cases}. \quad (3.18)$$

In addition, by considering a general interruption vacation case, we further define a stochastic matrix Q with the element $Q_{j',j}$ referring to the probability that the service of a packet will resume in phase j after the server returns from the interruption vacation, given that the service was interrupted at phase j' at the start of the vacation. Besides, we assume a single vacation, i.e., when the server returns from a vacation, it will start to offer services immediately if there are packets available in the system, or wait for arrivals of new packets and then begin to serve.

3.2.3 Over-deadline Dropping Principle with Instantaneous Delay Constraints

Body sensors have very limited storage and communication abilities due to their small physical sizes and stringent energy constraints. Thus, sensors need to make full use of their finite energy by transmitting the most valuable and emergent data, especially when the transmission channel suffers from human body effects. As we discussed in Section I, different from conventional sensor networks, whose objective is commonly aimed at

maximizing the system throughput under the average delay constraints, in WBANs, we focus more on maximize the valuable packets' transmissions under a instantaneous delay constraint. Thus, in order to ensure the timeliness of served packets and avoid energy waste for transmitting valueless packets, we need to carefully design the service principle.

Different from the traditional wireless communications, in WBANs, the packet suffering from long waiting time becomes less valuable than newly arrived packets [43]. Therefore, in contrast to the widely used earliest deadline transmission policy [64], packets with long waiting time should be dropped, such that important packets can be transmitted with shorter delay and the transmission energy for these valueless packets can be saved. On the other hand, since the chronological order of sensed data is also valuable information for the diagnosis of patients' medical conditions, the packets' transmission should also obey a first-come-first-service (FCFS) fashion. By jointly considering these two completely distinct requirements, the designed energy-saving service principle, named as the over-deadline dropping principle, is summarized as follows.

- The system follows a FCFS service discipline.
- Over-deadline dropping: The waiting time of all buffered packets will be examined at the beginning of each time slot and a packet will be dropped if its waiting time in the queue has exceeds its instantaneous delay constraint.

In practice, these delay limits for various packets sensed from different types of sensors can be predefined by referring to the real application requirements or recommended QoS requirements in standard IEEE 802.15.6. Since the packets services at a same sensor node are homogeneous, the underlying processes and parameters for all packets are the same, i.e., all packets in the queue are statistically identical. In addition, we assume infinite buffer size at the sensor nodes.

Obviously, with our designed over-deadline dropping principle, the server should constantly examine the waiting time of all buffered packets and discard the long-awaited packets that exceed their instantaneous delay constraints. However, such real-time

detection requirement makes the queueing analysis very complicated. By considering the fact that the head of line (HOL) packet in the queue always has the longest waiting time under the FCFS principle, the over-deadline dropping principle can be modeled by the HOL packet dropping (HOL-PD) principle. Nevertheless, the queueing model with the HOL-PD principle is still too difficult to be analyzed directly because of the HOL packet dropping process and instantaneous delay tracking. In the next section, we will explore the tail behavior of the delay distributions, and transform the HOL-PD principle into a buffer-overflowing principle.

3.3 Queueing Analysis

In this section, we develop a buffer-overflowing queueing principle to approximate the over-deadline principle by finding the optimal buffer length, and then the newly formulated queueing model is analyzed in details.

3.3.1 Buffer-overflowing Approximation

Inspired by the fact that the queueing length can indicate waiting time to some extent, we develop a buffer-overflowing principle to approximate the over-deadline principle through analyzing the tail probability of the waiting time in the queue. The new buffer-overflowing queueing model has the same queueing elements as the over-deadline queueing model, except a finite buffer length and the packet dropping principle, i.e., the HOL packet will be dropped when a new packet arrives in the already fully-occupied buffer. The approximation error between these two principles can be minimized when for the majority of served packets, their instantaneous waiting delay under the buffer-overflowing dropping principle is strictly less the deadline (i.e., instantaneous delay constraint). Therefore, by further considering the objective to maximize the system throughput (i.e., minimize the packet transmission failure probability), we aim at looking for an optimal buffer size L^* to minimize the tail probability of packet waiting time distribution for served packets that

exceed their delay limits. Such optimization problem can be formulated as follows,

$$L^* = \arg \min_{L \in \mathcal{Z}} (P_{tf}(L) + \sum_{i=t_{bnd}+1}^{\infty} W_i(L)) \quad (19)$$

s.t. $L \in [1, L_{bnd}]$,

where t_{bnd} is the predefined limit of packet waiting time. $P_{tf}(L)$ and $W_i(L)$ represent the packet transmission failure probability and waiting time distribution when the buffer size is L , respectively. \mathcal{Z} denotes the set of integers and L_{bnd} denotes the largest buffer size. Note that the queueing system changes with respect to the buffer size, and the close-form expressions for packet waiting time distribution and transmission failure probability are commonly not available. Owing to the finite solution space, we can adopt heuristic direct search techniques, such as the Hooke and Jeeves direct search method [65], to find the optimal buffer length.

However, obtaining the packet transmission failure probability and waiting time distribution requires deriving the queue length stationary distribution, which will result in high computational complexity. Optionally, we propose an approximation method to find the optimal solution with low complexity. Let \mathbf{C}_1 denote the event that the maximum waiting time of served packets in the queue is larger than t_{bnd} , and \mathbf{C}_2 denote the event that the minimum waiting time of dropped packets is less than t_{bnd} . \mathbf{C}_1 and \mathbf{C}_2 can indicate the proportion of valueless packets (i.e. exceed the limit) in the served packets and the proportion of valuable packets in the dropped packets, respectively. Obviously, the optimal buffer length should make both events \mathbf{C}_1 and \mathbf{C}_2 less likely to happen, i.e., $Pr\{\mathbf{C}_1|L^*\} \rightarrow 0$ and $Pr\{\mathbf{C}_2|L^*\} \rightarrow 0$. Hence, we formulate a new optimization problem as

$$L^* = \arg \min_{L \in \mathcal{Z}} (Pr_1 + Pr_2) \quad (20)$$

s.t. $L \in [1, L_{bnd}]$,

where $Pr_1 = Pr_{rob}\{\mathbf{C}_1|L\}$ and $Pr_2 = Pr_{rob}\{\mathbf{C}_2|L\}$. Since the packet dropping only happens

when the buffer is full and at most one packet arrives in each slot, the optimal buffer size must be less than t_{bnd} , so that we can set $L_{bnd} = t_{bnd}$. In addition, it is obvious that a higher Pr_1 will make more served packet become valueless (i.e., breaking the delay limit) and a higher Pr_2 will increase the packet transmission failure probability. Intuitively, these two probabilities corresponds to the tail probability and transmission failure probability in the original optimization problem receptively. Next, we focus on the derivation of these two probabilities.

We first define the packets that suffer the longest waiting periods in the buffer but get served eventually as *Late Packets* [43]. Since the maximum waiting time means the worst case, the distribution of maximum waiting time can be approximately indicated by the waiting duration that *Late Packets* experience and the corresponding probabilities. Specifically, the queueing behavior of such a *Late Packet* can be separated into three periods : 1) waits t_1 time slots until it becomes the HOL packet and all the ahead packets are dropped due to over-deadline; 2) just stays at the HOL position for t_2 time slots without any packet arrivals and departures in the system; 3) leaves the queue buffer and starts to get service just before a new packet arrives. Accordingly, the waiting time distribution of such a *Late Packet*, denoted by ω_j , can be derived as

$$\omega_j = \sum_{t=L-1}^{j-1} Pb_1(t)Pb_2(j-t), j = t_1 + t_2 + 1, \quad (3.21)$$

with

$$Pb_1(t) \simeq \binom{t-1}{L-2} \boldsymbol{\pi} [(D_1)^{L-1} (D_0)^{t-L+1}] \mathbf{1} \quad (3.22)$$

$$Pb_2(t) \simeq (\boldsymbol{\pi} D_0^{t-1} D_1 \mathbf{1}) \sum_{k=1}^t P_s(k) \left(1 - \sum_{m=0}^{k-1} P_f(m)\right) P_v(t-k) \quad (3.23)$$

where $Pb_1(t)$ and $Pb_2(t)$ are the corresponding probabilities of first period and following

two periods respectively. Consequently, the probability Pr_1 can be calculated as

$$Pr_1 \simeq 1 - \sum_{j=L}^{t_{bnd}} \omega_j. \quad (3.24)$$

Similarly, the minimum waiting time of dropped packets can be approximated by the waiting duration for those arrival packets that are dropped as early as possible, which are defined as *Early Dropped Packets*. Such a *early dropped packet* is dropped due to the busy arrival packets. Thus, Pr_2 can be calculated as

$$Pr_2 \simeq \sum_{i=L}^{t_{bnd}} \binom{i-1}{L-1} \pi[(D_1)^L (D_0)^{i-L}] \mathbf{1}. \quad (3.25)$$

Although the actual tail behaviors cannot be fully described by equations (3.24) and (3.25), if a served packet holds a very long waiting time, it is most likely be of a *Late Packet*. In other words, the *late packets* dominate the calculation of the maximum waiting time distribution. Likewise, the *Early dropped packet* accounts most for the minimum waiting time of dropped packets. These ideas are verified through extensive simulations in Chapter 3.4.

3.3.2 Matrix-Geometric Analysis

In the long run, HOL packet dropping principle is equivalent to the end-of-the-line (EOL) packet dropping principle. This is because i) packet dropping occurs only if the buffer is fully occupied, which is same for both principles, and hence HOL and EOL will have identical packet dropping probability; ii) all the packets sensed from the same sensor are statistically identical. Thus the only difference between these two principles is that dropped packets under HOL hold some waiting delay while dropped packets under EOL do not. However, the dropped packets under either EOL or HOL won't affect the waiting time for those packet that get served eventually. Thus the difference has no influence on analyzing the performance of these served packets. Therefore, after deriving the optimal buffer length L^* , the queueing model is reformulated as a discrete-time queue with buffer-overflowing

block matrices are explained in details below.

Matrix B stands for the scenario that the packet number remains unchanged because there is no new packet departure and no new arrival. It can be further represented as

$$B = \begin{bmatrix} B^{s,s} & B^{s,v} \\ B^{v,s} & B^{v,v} \end{bmatrix}, \quad (3.27)$$

where $B^{s,s} = T \otimes D_0$ represents the situation that there is no new packet arrival and the service is effective while the system remains empty. The operator \otimes denotes the Kronecker Product. $B^{s,v} = \mathbf{t} \otimes D_0 \otimes \phi$ represents the situation that the server is blocked and goes to a vacation with no new arrival and no packet in the system. $B^{v,s} = \alpha \otimes D_0 \otimes \mathbf{v}$ represents that the system remains empty without any new arrival while the vacation period ends and the server becomes effective in the current time slot. Lastly, $B^{v,v} = D_0 \otimes V$ represents the situation that the system remains empty and the server continues on vacation without any new arrival.

Matrix A_1 represents the scenario that the number of packets in the system is unchanged in two consecutive time slots due to either no packet arrival and departure, or one packet departure and one packet arrival. Obviously, A_1 is the general case of B and can be represented as

$$A_1 = \begin{bmatrix} A_1^{s,s} & A_1^{s,v} \\ A_1^{v,s} & A_1^{v,v} \end{bmatrix}, \quad (3.28)$$

where

- $A_1^{s,s} = T \otimes [D_0 \otimes S + D_1 \otimes (\mathbf{s}\beta)]$, denotes cases that i) there is no new packet arrival and the server is still effective without any packet departure, or ii) there is one new packet arrival while the server remains effective as one packet is served.
- $A_1^{s,v} = \mathbf{t} \otimes [D_0 \otimes \phi \otimes S^* + D_1 \otimes \phi \otimes (\mathbf{s}e_1^T(n_s + 1))]$, denotes cases that i) the effective period of the server ended and the vacation period starts without any packet arrival or departure, or ii) there is one packet arrival and one packet departure as the server

begins a vacation at the ends of this time slot.

- $A_1^{v,s} = \alpha \otimes D_0 \otimes \mathbf{v} \otimes Q^*$, represents the situation that the server returns from a vacation and begins to offer service without any packet arrival and departure.
- $A_1^{v,v} = D_0 \otimes V \otimes I_{n_s+1}$, represents the situation that there is no new packet arrival and the server continues on vacation.

Note that $S^* = [0 \ S]$ of $n_s \times (n_s + 1)$, $Q^* = [\beta \ Q]^T$, e_j denotes the j th column of an identity matrix, and the super script $(\cdot)^T$ represents the matrix transpose.

Matrix E stands for the scenario that the system becomes empty after a packet is successfully served without new packet arrival. Specifically, it can be represented as

$$E = \begin{bmatrix} E^{s,s} & E^{s,v} \\ E^{v,s} & E^{v,v} \end{bmatrix}, \quad (3.29)$$

where $E^{s,s} = T \otimes D_0 \otimes \mathbf{s}$ represents the case that there is no new packet arrival and the service is still effective after one packet was served, while the system becomes empty at the end of this time slot. Submatrix $E^{s,v} = \mathbf{t} \otimes D_0 \otimes \phi \otimes \mathbf{s}$ represents the case that there is a packet departure without any new arrival and the server is blocked and goes to a vacation. Since there cannot be any packet departure when the server is on vacation, we then have $E^{v,s} = \mathbf{0}$, $E^{v,v} = \mathbf{0}$.

Matrix A_2 represents the scenario that there is a packet departure and no new arrival, i.e., a typical death process. Intuitively, A_2 represents a general form of E and can be represented as

$$A_2 = \begin{bmatrix} A_2^{s,s} & A_2^{s,v} \\ A_2^{v,s} & A_2^{v,v} \end{bmatrix}, \quad (3.30)$$

with $A_2^{s,s} = T \otimes D_0 \otimes (\mathbf{s}\beta)$, $A_2^{s,v} = \mathbf{t} \otimes D_0 \otimes \phi \otimes (\mathbf{s}e_1^T(n_s + 1))$ and $A_2^{v,s} = A_2^{v,v} = \mathbf{0}$.

Matrix A_0 represents a birth process, i.e., there is a new packet arrival without any packet served. The birth process consists of the following four cases: i) there is a new packet entering the non-empty system, while the server fails offering a successful service

but keeping at the effective state; ii) the service is interrupted and the server goes to a vacation with a new packet arrival; iii) there is a new packet arrival and the server becomes effective after returning from an interruption vacation; and iv) there is one new packet arrival but the server remains on vacation. In summary, the transition submatrix A_0 can be represented as

$$A_0 = \begin{bmatrix} T \otimes D_1 \otimes S & \mathbf{t} \otimes D_1 \otimes \phi \otimes S^* \\ \alpha \otimes D_1 \otimes \mathbf{v} \otimes Q^* & D_1 \otimes V \otimes I_{n_s+1} \end{bmatrix}. \quad (3.31)$$

Matrix C represents the special case of A_0 when the system starts with a empty state, and can be represented as

$$C = \begin{bmatrix} T \otimes D_1 \otimes \beta & \mathbf{t} \otimes D_1 \otimes \phi \otimes e_1^T(n_s + 1) \\ \alpha \otimes D_1 \otimes \mathbf{v} \otimes \beta & D_1 \otimes V \otimes e_1^T(n_s + 1) \end{bmatrix}. \quad (3.32)$$

3.3.3 Stationary Distribution

Since the transition matrix P belongs to a finite quasi-birth-death (QBD) type, we apply the matrix-geometric method to analyze the steady-state distribution. Let \mathbf{x} denote the stationary queue length distribution. Then, we have

$$\mathbf{x} = \mathbf{x}P, \mathbf{x}\mathbf{1} = \mathbf{1}, \quad (3.33)$$

where

$$\begin{aligned} \mathbf{x} &= [\mathbf{x}_0, \mathbf{x}_1, \dots, \mathbf{x}_L^*], \mathbf{x}_0 = [\mathbf{x}_0^s, \mathbf{x}_0^v], \mathbf{x}_i = [\mathbf{x}_i^s, \mathbf{x}_i^v], i \geq 1 \\ \mathbf{x}_i^v &= [\mathbf{x}_{i,1}, \mathbf{x}_{i,2}, \dots, \mathbf{x}_{i,k}, \dots, \mathbf{x}_{i,n_a}], \mathbf{x}_i^s = [\mathbf{x}_{i,1}, \mathbf{x}_{i,2}, \dots, \mathbf{x}_{i,u}, \dots, \mathbf{x}_{i,n_b}], \\ \mathbf{x}_{i,k}^v &= [\mathbf{x}_{i,k,1}, \mathbf{x}_{i,k,2}, \dots, \mathbf{x}_{i,k,l}, \dots, \mathbf{x}_{i,k,n_v}], \mathbf{x}_{i,u}^s = [\mathbf{x}_{i,u,1}, \mathbf{x}_{i,u,2}, \dots, \mathbf{x}_{i,u,k}, \dots, \mathbf{x}_{i,u,n_a}], \\ \mathbf{x}_{i,k,l}^v &= [x_{i,k,l,1}, x_{i,k,l,2}, \dots, x_{i,k,l,n_s}], \mathbf{x}_{i,u,k}^s = [x_{i,u,k,1}, x_{i,u,k,2}, \dots, x_{i,u,k,n_s}], \\ \mathbf{x}_0^v &= [\mathbf{x}_{0,1}^v, \mathbf{x}_{0,2}^v, \dots, \mathbf{x}_{0,k}^v, \dots, \mathbf{x}_{0,n_a}^v], \mathbf{x}_{0,k}^v = [x_{0,k,1}, x_{0,k,2}, \dots, x_{0,k,n_v}], \\ \mathbf{x}_0^s &= [\mathbf{x}_{0,1}^s, \dots, \mathbf{x}_{0,u}^s, \dots, \mathbf{x}_{0,n_b}^s], \mathbf{x}_{0,u}^s = [x_{0,u,1}^s, \dots, x_{0,u,k}^s, \dots, x_{0,u,n_a}^s], \mathbf{x}_{0,u,k}^s = [x_{0,u,k,1}, \dots, x_{0,u,k,n_s}]. \end{aligned}$$

According to [66], the stationary distribution \boldsymbol{x} has the following structure,

$$\boldsymbol{x}_i = \eta_1 R_1^{i-1} + \eta_2 R_2^{L^*-i}, i \geq 1, \quad (3.34)$$

where η_1 and η_2 are two constant vectors. R_1 and R_2 are the unique minimal non-negative solutions of following quadratic matrix equations, respectively,

$$R_1 = A_0 + R_1 A_1 + R_1^2 A_2, \quad (3.35)$$

$$R_2 = A_2 + R_2 A_1 + R_2^2 A_0. \quad (3.36)$$

Matrices R_1 and R_2 can be solved by using the cyclic reduction (CR) method [62]. Given R_1 and R_2 , the boundary value \boldsymbol{x}_0 and the two constant vectors η_1, η_2 can be obtained by solving the following equations

$$\begin{cases} [\boldsymbol{x}_0, \eta_1, \eta_2] = [\boldsymbol{x}_0, \eta_1, \eta_2] \Gamma[R_1, R_2], \\ \boldsymbol{x}_0 \mathbf{1} + (\eta_1 \Lambda_1 + \eta_2 \Lambda_2) \mathbf{1} = 1, \end{cases} \quad (3.37)$$

where

$$\Lambda_1 = \sum_{i=0}^{L^*-1} R_1^i, \quad \Lambda_2 = \sum_{i=0}^{L^*-1} R_2^i, \quad (3.38)$$

$$\Gamma[R_1, R_2] = \begin{bmatrix} B & C & 0 \\ E & A_1 + R_1 A_2 & R_1^{L^*-2} [A_0 + R_1 (A_0 + A_1) - R_1] \\ R_2^{L^*-1} E & R_2^{L^*-2} (A_2 + R_2 A_1 - R_2) & R_2 A_0 + A_0 + A_1 \end{bmatrix}. \quad (3.39)$$

Obviously, $[\boldsymbol{x}_0, \eta_1, \eta_2]$ is the left-invariant eigenvector of $\Gamma[R_1, R_2]$ with normalization to make the probabilities sum up to unity. Then, according to equation (3.34), the stationary distribution can be obtained accordingly.

3.3.4 Performance Metrics

Based on the derived stationary distribution, system performance in terms of the average queue length, packet transmission failure probability, queue throughput, and average delay can be analyzed as follows.

Average Queue Length

According to the server states (i.e., working and vacation), the average number of packets in the system equals

$$\bar{x} = \sum_{i=1}^{L^*} i(\mathbf{x}_i \mathbf{1}) = \sum_{i=1}^{L^*} i(\mathbf{x}_i^s \mathbf{1} + \mathbf{x}_i^v \mathbf{1}). \quad (3.40)$$

Let $\bar{x}_s = \sum_{i=1}^{L^*} i(\mathbf{x}_i^s \mathbf{1})$, and $\bar{x}_v = \sum_{i=1}^{L^*} i(\mathbf{x}_i^v \mathbf{1})$. Then we have, $\bar{x} = \bar{x}_s + \bar{x}_v$. Note that \bar{x}_s and \bar{x}_v denote the expected number of packets in the system during the server working period and the server vacation period, respectively. They can be calculated as follows

$$\bar{x}_s = \sum_{i=1}^{L^*} i(\mathbf{x}_i^s \mathbf{1}) = \sum_{i=1}^{L^*} \sum_{u=1}^{n_b} \sum_{k=1}^{n_a} \sum_{j=1}^{n_s} i x_{i,u,k,j}, \quad (3.41)$$

$$\bar{x}_v = \sum_{i=1}^{L^*} i(\mathbf{x}_i^v \mathbf{1}) = \sum_{i=1}^{L^*} \sum_{k=1}^{n_a} \sum_{l=1}^{n_v} \sum_{j'=1}^{n_s} i x_{i,k,l,j'}. \quad (3.42)$$

By removing the packet under service, the average queue length can be obtained by

$$\bar{x}_q = \sum_{i=2}^{L^*} (i-1) \mathbf{x}_i \mathbf{1}. \quad (3.43)$$

Transmission Failure Probability

A buffered packet will be dropped if its waiting time in the queue reaches the delay limit (i.e., becomes valueless). Such packet dropping has been transformed into buffer-overflowing dropping, where the HOL packet will be dropped if the queue buffer is full and a new packet arrives. Thus, the queueing dropping probability can be calculated as

$$P_{dr} = \mathbf{x}_{L^*+1} \mathbf{1}. \quad (3.44)$$

Besides, the packet under service can also be blocked when its re-transmission times are larger than the retry limit. Thus, the blocking probability can be represented as

$$P_{bl} = (1 - P_{dr})\rho_d. \quad (3.45)$$

In summary, we define a packet transmission failure probability P_{tf} as the probability that the transmission of a sensed packet is failed due to either over-deadline (i.e., dropped) or over-retry (i.e., blocked). It can be obtained as

$$P_{tf} = P_{dr} + P_{bl}. \quad (3.46)$$

Queue throughput

If a packet is neither blocked nor dropped under service, it will be successfully transmitted in the end. Therefore the queue throughput, defined as the expected number of effectively served packets, can be obtained as

$$\varepsilon = \lambda(1 - P_{tf}), \quad (3.47)$$

where λ denote the average discrete arrival rate, and can be obtained as $\lambda = (\boldsymbol{\pi} D_1^{-1} \mathbf{1})^{-1}$.

Average waiting delay and average access delay

The average waiting delay of a served packet \bar{W} is defined as the number of time slots from its arrival to when it starts to receive service. The average access delay \bar{d} is the mean system time from a packet's arrival to its departure, and equals the waiting delay plus the time to receive service. By using Little's Law, we have

$$\bar{W} = \frac{\bar{x}_q}{\varepsilon}, \quad (3.48)$$

$$\bar{d} = \frac{\bar{x}}{\varepsilon}. \quad (3.49)$$

Waiting time distribution

Since this buffer-overflowing queue has a finite buffer, a packet cannot receive services if it arrives to find the buffer full. We only focus on those packets that can be served eventually. Under the EOL packet dropping principle, the waiting time of an undropped packet equals the service duration of all the packets ahead of it. Furthermore, for a new arrival packet, the probability that there are m packets ahead of it in the system is $\frac{\mathbf{x}_m \mathbf{1}}{1 - \mathbf{x}_{L^*+1} \mathbf{1}}$, $m \leq L^*$. To analyze the waiting time distribution, we construct an absorbing Markov chain to represent the departure process of ahead packets with transient states $\{(m, u, j), (m, l, j')\}$, $m > 0$, and the absorbing state $\{m = 0\}$. Define U as the sub-stochastic matrix representing the transient state transitions. Then U can be written as

$$U = \begin{bmatrix} F & & & & & \\ G & F & & & & \\ & G & F & & & \\ & & & \ddots & \ddots & \\ & & & & G & F \end{bmatrix}, \quad (3.50)$$

where

$$F = \begin{bmatrix} T \otimes S & \mathbf{t} \otimes \phi \otimes S^* \\ \alpha \otimes \mathbf{v} \otimes Q^* & V \otimes I_{n_s+1} \end{bmatrix}, G = \begin{bmatrix} T \otimes (\mathbf{s}\beta) & \mathbf{t} \otimes \phi \otimes (\mathbf{t}e_1^T(n_s + 1)) \\ 0 & 0 \end{bmatrix}. \quad (3.51)$$

Moreover, the initial state vector σ can be obtained as, $\sigma = (1 - \mathbf{x}_{L^*+1} \mathbf{1})[\mathbf{x}_1, \mathbf{x}_2, \dots, \mathbf{x}_{L^*}]$. Following the formulated absorbing Markov chain, the waiting time distribution W_i can be calculated as

$$W_i = \begin{cases} (1 - \mathbf{x}_{L^*+1} \mathbf{1})\mathbf{x}_0 \mathbf{1}, & i = 0 \\ \sigma U^{i-1} \mathbf{u}, & i \geq 1 \end{cases}, \quad (3.52)$$

where $\mathbf{u} = \mathbf{1} - U\mathbf{1}$.

3.4 Numerical and Simulation Results

In this section, we analyze the system performance of IEEE 802.15.6-based WBANs and verify our proposed analytical framework via extensive simulations. The impacts of the human body shadowing and instantaneous delay limit on the performance are also investigated.

3.4.1 Simulation Parameters

We consider a CAMS/CA based uplink transmission scenario in a star-topology WBAN with $N = 8$ sensors and a coordinator. Each sensor corresponds to one specific type of traffic loads with different contention window sizes. Here, we take one medical sensor node as an example for the performance evaluation, and the maximum re-transmission limit for a medical packet is set as $R = 3$. The arrival process is modeled by a MAP distribution with the following parameters:

$$D_0 = (I - a\Lambda) \begin{bmatrix} 0.1 & 0.9 \\ 0.2 & 0.8 \end{bmatrix}, \quad D_1 = a\Lambda \begin{bmatrix} 0.1 & 0.9 \\ 0.2 & 0.8 \end{bmatrix}, \quad (3.53)$$

where $a\Lambda$ is a diagonal matrix representing the arrival rate at each phase. In our simulation, we set $\Lambda = \begin{bmatrix} 0.12 & 0 \\ 0 & 0.15 \end{bmatrix}$ and vary a from 1 to 3 to indicate different arrival traffic intensities. The packet error rate is set as $\bar{P}_e = 0.08$. Consequently, the matrices of the PH model for the service process can be obtained by equations 3.10 and 3.13

$$S = \begin{bmatrix} 0.2897 & 0.0568 & 0 & 0 \\ 0 & 0.2897 & 0.0568 & 0 \\ 0 & 0 & 0.3759 & 0.0499 \\ 0 & 0 & 0 & 0.3759 \end{bmatrix}, \quad \mathbf{s} = \begin{bmatrix} 0.6535 \\ 0.6535 \\ 0.5742 \\ 0.6241 \end{bmatrix}, \quad (3.54)$$

and the dropping rate $\rho_d \simeq 0.0028$. In our simulation, we assume the packet service will resume from the state where the service is interrupted, i.e. matrix Q is an identity matrix. Moreover, as for the shadowing interruption, we consider a geometric distribution as a

Table 3.1: The verification of queue length stationary distribution under different arrival intensities

Queue length	$a = 1$		$a = 1.5$		$a = 2$	
	OD(sim)	BO(analysis)	OD(sim)	BO(analysis)	OD(sim)	BO(analysis)
0	63.8590	65.1080	49.4520	49.1210	33.4770	33.4710
1	25.6220	25.2060	30.1240	29.8200	29.0500	29.1960
2	7.2300	6.6260	11.5390	11.5260	15.0660	14.8820
3	2.2600	2.1260	4.7930	5.2000	8.9730	8.6100
4	0.7020	0.6400	2.2520	2.3660	5.4830	5.5510
5	0.2320	0.2310	0.9910	1.0670	3.4390	3.3250
6	0.0720	0.0480	0.4990	0.5340	2.0030	2.1090
7	0.0220	0.0130	0.2070	0.2090	1.2570	1.2460
8	0.0010	0.0020	0.1200	0.1230	0.6570	0.6740
9	0.0000	0.0000	0.0210	0.0308	0.3560	0.3970
10	0.0000	0.0000	0.0020	0.0032	0.1620	0.2420
11	0.0000	0.0000	0.0000	0.0000	0.0530	0.1730
12	0.0000	0.0000	0.0000	0.0000	0.0210	0.0860
13	0.0000	0.0000	0.0000	0.0000	0.0030	0.0340
14	0.0000	0.0000	0.0000	0.0000	0.0000	0.0040
P_{tf}	0.0038	0.0042	0.0049	0.0054	0.0066	0.0070

special case of PH distribution with single phase [67]: $\alpha = 1$, $T = 1 - w_p$, $\mathbf{t} = w_p$, $\phi = 1$, $V = 1 - v_q$, $\mathbf{v} = v_q$. By default, we set $w_p = 0.1$ and $v_q = 0.3$ in the evaluation.

Note that some of the above parameters may vary depending on different evaluation scenarios and specific parameter settings won't affect the observation results. We develop a time-driven simulator in Matlab to evaluate over-deadline scenarios with different settings. For each parameter setting, we conduct 5 simulations and the time length of each simulation is 10^6 slots. A Matlab toolbox on matrix analytic methods developed by Bini et al. in [68] is used to solve the QBD Markov chain.

3.4.2 Queueing Dynamics Verification

Table 3.1 shows the comparison of the stationary queue length distribution obtained through simulation under the over-deadline (OD) principle with that obtained through approximated theoretical analysis under the buffer-overflowing (BO) principle. It can be seen that both results are very close under different arrival intensities, $a = 1$, $a = 1.5$ and $a = 2$. Moreover, we can see that the packet transmission failure probability obtained through

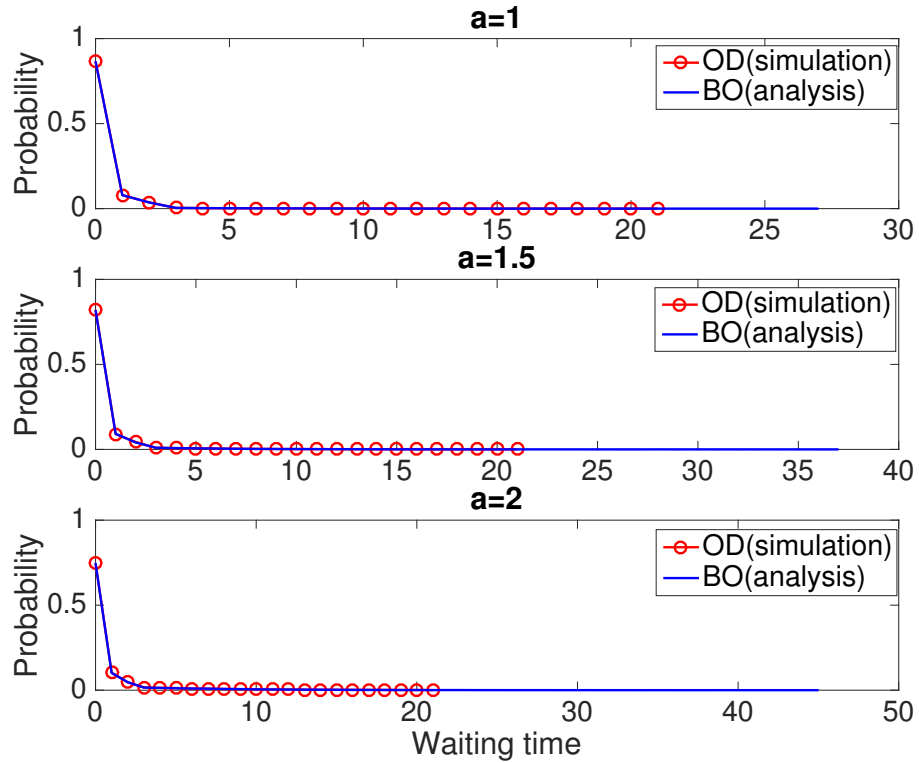


Figure 3.4: The verification of packet waiting time distribution under different arrival intensities

simulation is also close to the analytical results, which further verifies the accuracy of our proposed analytical framework and the validity of our buffer-overflowing approximation. Note that when $a = 2$, the maximum queue length of the analytical result is 14 while that of the simulation result is 13. This is because the buffer size is constrained to an integer, so that the optimal buffer length in our buffer-overflowing approximation may sometimes be greater or less than the buffer size of simulation results by one. However, as the table shows, the approximation only results in slight differences.

Fig. 3.4 compares the average waiting delay between simulation and analytical results with respect to the arrival intensity. From the figure, we can see that the maximum waiting time of the OD simulation results is always fixed at the instantaneous delay limit (20 slots) while that of the BO analytical results is greater than 20 slots and varies with arrival intensities. However, we have to point out that the BO analytical results are very close to the OD simulation results and the probabilities that the waiting time is larger

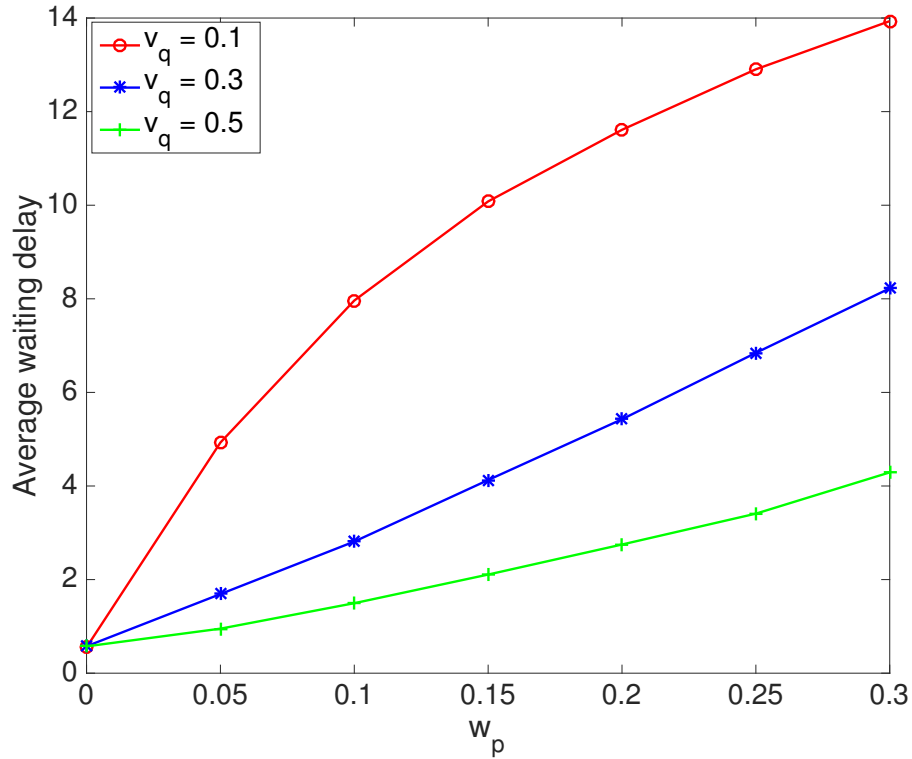


Figure 3.5: The effect of shadowing interruption on the average waiting delay

than the instantaneous delay limit only contribute less than 0.0001 in total. Therefore, our proposed analytical framework can provide accurate and computationally efficient analyses on system performance by jointly considering instantaneous delay constraints and shadowing interruptions.

3.4.3 Impacts of Body Shadowing Interruption

We investigate the effect of the human body shadowing interruption on the system performance under different working and vacation probabilities. Fig. 3.5 shows the average waiting delay changes with respect to the probability w_p that the service becomes invalid and vacation starts, and the probability v_q that the vacation ends and the service resumes. From the figure, we can observe that the average waiting delay increases as the probability w_p increases, which is because a larger w_p means the service will be interrupted more frequently. With the fixed w_p , the waiting delay decreases as the probability v_q increases.

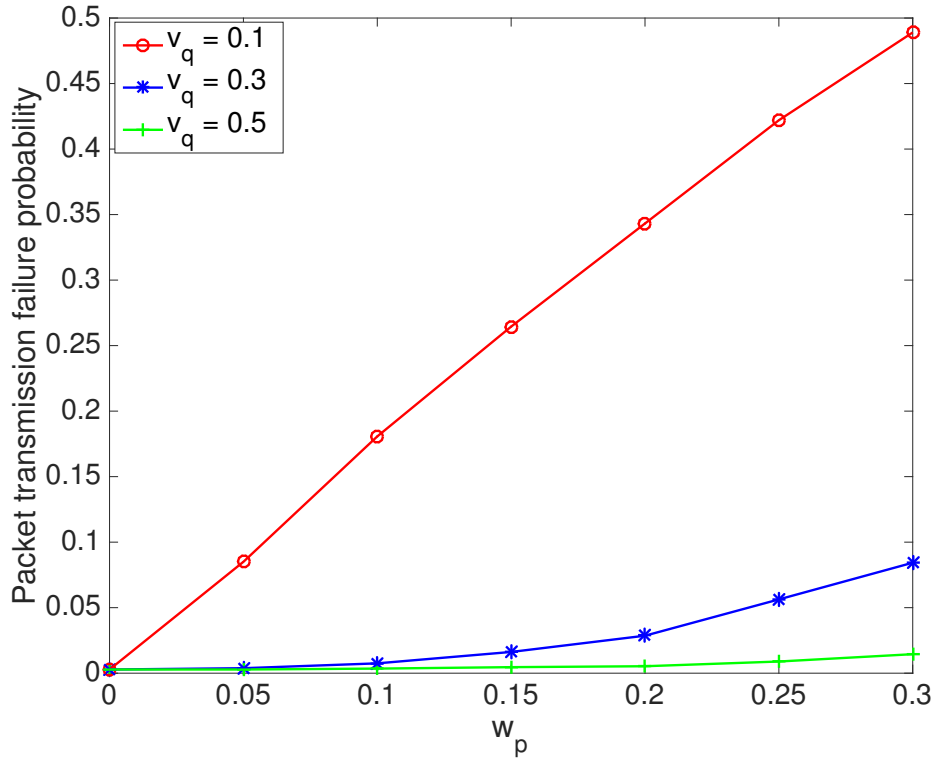


Figure 3.6: The effect of shadowing interruption on the transmission failure probability

This is because a larger v_q indicates the service is more likely to return from a vacation interruption.

The effect of shadowing interruption on the packet transmission failure probability is shown in Fig. 3.6. As expected, the failure probability increases when the working-interrupted probability w_p increases or the vacation-ending probability v_q decreases. Specially, when $w_p = 0$, the service is not affected by the human body shadowing, so that the system can achieve the best performance (i.e. the lowest waiting delay and transmission failure probability). Obviously, the body shadowing interruption causes great performance degradation for packet transmission with stringent instantaneous delay constraints.

3.4.4 Impacts of Instantaneous Delay Constraint

Fig. 3.7 and Fig. 3.8 demonstrate the effects of the instantaneous delay constraint on the average packet waiting delay and the transmission failure probability, respectively,

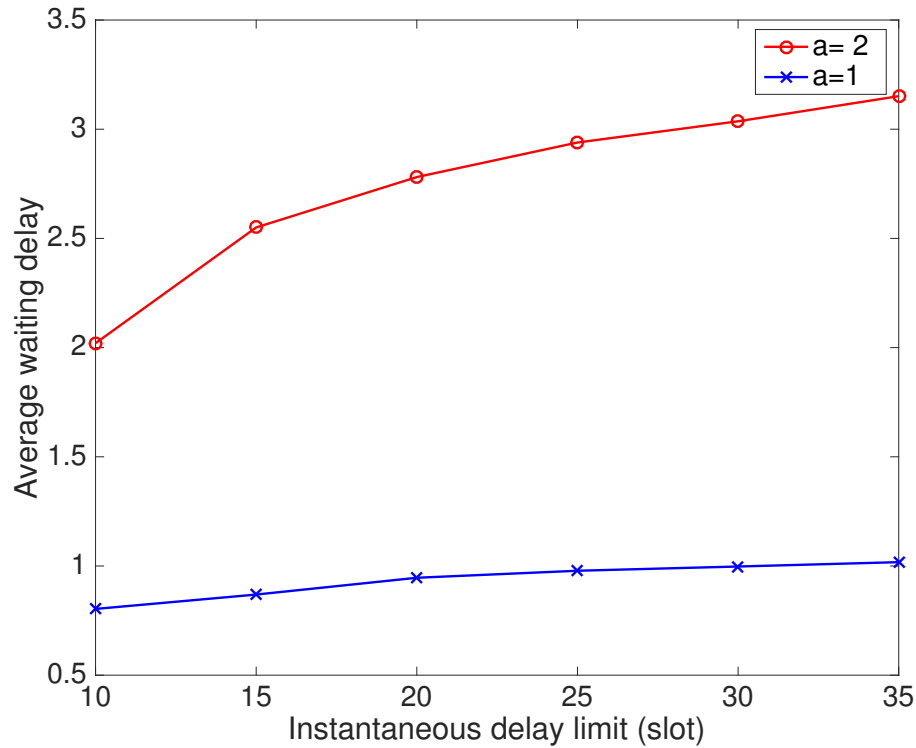


Figure 3.7: The effect of instantaneous delay limit on the average waiting delay

under two different traffic loads, $a = 1$ and $a = 2$. For both figures, the shadowing interruption is configured to be same with $w_p = 0.1, v_q = 0.3$. As shown in Fig. 3.7, the average waiting delay increases with the value of instantaneous delay limit. It is also noted that the average waiting delay is much smaller than the instantaneous delay limit. This is because the instantaneous delay limit represents the maximum waiting time of served packets. This observation clearly validate the existence of differences between average delay constraints and instantaneous delay constraints. In addition, a larger delay limit provides more transmission opportunities for long-waited packets, which leads to a lower packet transmission failure probability accordingly. It can be seen from Fig. 3.8 that the packet transmission failure probability decreases as the delay limit increases. Clearly, we can also observe that with a fixed delay limit, the higher arrival intensity results in a larger average waiting delay and a larger transmission failure probability.

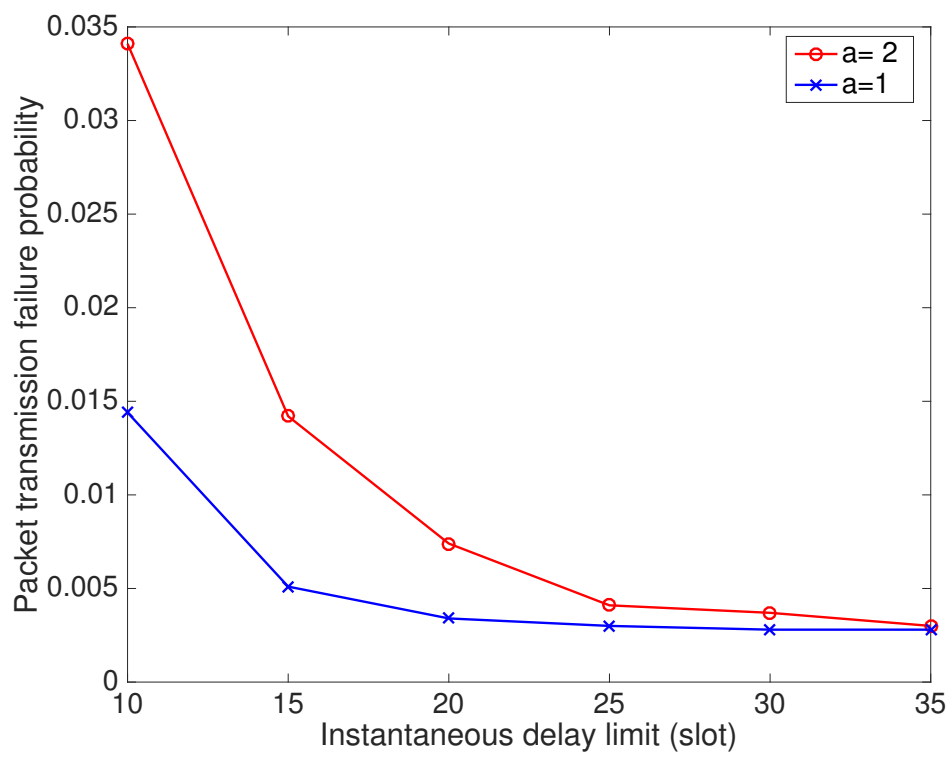


Figure 3.8: The effect of instantaneous delay limit on the transmission failure probability

Chapter 4

Energy Efficient Packet Transmission

Strategies for Wireless Body Area

Networks with Rechargeable Sensors

In this chapter, we investigate energy efficient packet transmission strategies for wireless body area networks (WBANs) with rechargeable sensors. For practical implementations, we propose a multi-threshold based transmission strategy by taking into account the channel state, battery state and number of buffered packets in the system. A discrete Markov arrival process (DMAP) is introduced to jointly model channel correlations and energy allocations. After that, with given thresholds and corresponding energy allocations, a level dependent Quasi-Birth-and-Death Markov chain is constructed to evaluate the system performance. According to the derived performance metrics, we formulate an optimization problem to find optimal thresholds for energy efficiency maximization with reasonable performance provisioning. Extensive simulations are conducted to verify our proposed queueing analytical model and demonstrate performance gains of our proposed strategy in WBANs over counterparts.

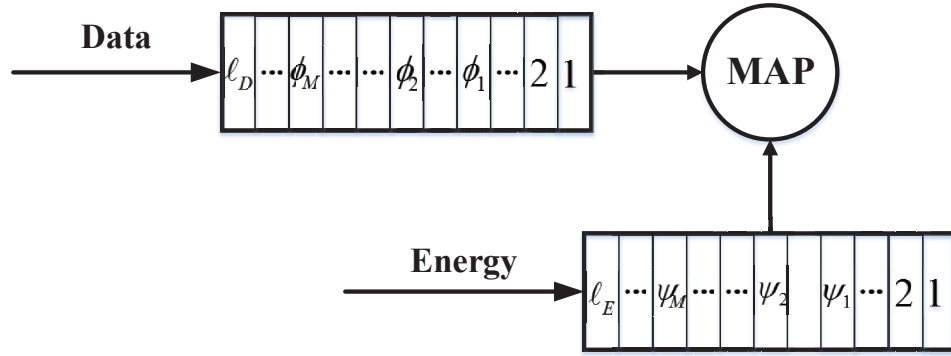


Figure 4.1: Threshold-based queueing system under study

4.1 System Model

4.1.1 Network Model

We consider a star-topology WBAN, where each sensor node is capable of recharging its capacity-limited battery from human bodies or external energy sources in the surrounding environment. The harvesting process is independent from data transmission, and each sensor node can transmit data and collect energy simultaneously.

The time is divided into slots with equal lengths. Each data packet needs at least one time slot for transmission and there is at most one new packet arrival in a slot. We quantize the battery energy into discrete units, and assume that at least one unit of energy is required to transmit one packet [69]. Initially, each sensor node stored E_0 units of energy and new units of energy are randomly collected when the battery is not full. The service of the node will be suspended if the battery is depleted, and will be restarted until new energy is harvested.

4.1.2 Channel Model

The fading channel around human bodies are correlated [52] and IEEE standard 802.15.6 [45] suggested the use of Markov channel models for WBANs. Like [70], we consider a slow-fading channel where the instantaneous channel gain h remains the same in a slot,

but it may change slot by slot. Through partitioning the range of channel gain into K intervals, the channel is modeled as a finite state Markov chain (FSMC) and the state space is denoted as $S = \{s_1, s_2, \dots, s_K\}$. The transition probability $P_{i,j}$, $i, j \in \{1, 2, \dots, K\}$, from state i to j can be obtained from practical measurements or statistical models [70]. Since the correlations only exist between adjacent states, we have $P_{i,j} = 0$, if $|i - j| > 1$.

4.1.3 Queueing Model

A sensor node has two queues to store data and energy arrivals, respectively. The data queue has a finite buffer length ℓ_D and the energy queue has a buffer length of ℓ_E . Both queues follow a first come first served fashion, and the service of one packet requires at least one unit of energy. In this discrete-time system, we model packet arrivals and energy arrivals by Bernoulli processes with probabilities α and β , respectively. The queueing structure of the system under study at a sensor node is illustrated in Fig. 4.1.

In the channel model, the packet error rate $\epsilon_i(\theta)$ at the i th state is dependent on the allocated amount of transmission energy in one slot, θ . Since energy allocations in our strategy are adaptively adjusted based on the status of data buffer and energy battery, we construct an absorbing Markov chain to model the service process which jointly considers the channel characteristics and energy allocations. Let $S' = \{s_0, S\}$ denote the state space of the absorbing chain, where the absorbing state s_0 represents the successful packet transmission, i.e., a successful departure. Then a discrete Markov arrival process is introduced to model the absorbing Markov chain, and can be represented by a matrix pair (D_0, D_1) , where both matrices have an order of K equal to the number of non-absorbing states. The elements $(D_0)_{ij}$ and $(D_1)_{ij}$ represent the transition probabilities from state i to state j without and with a successful packet transmission (i.e., a packet departure), respectively, which can be derived by

$$(D_0)_{ij} = \epsilon_i(\theta)P_{i,j}, |i - j| \leq 1, \quad (4.1)$$

$$(D_1)_{ij} = (1 - \epsilon_i(\theta))P_{i,j}, |i - j| \leq 1. \quad (4.2)$$

For clarity, we use the matrix pair $(D_0(\theta), D_1(\theta))$ to represent the service processes with energy allocation θ .

Let $D = D_0 + D_1$. Then, the matrix D is stochastic and irreducible, and $D\mathbf{1} = \mathbf{1}$, where $\mathbf{1}$ represents a column vector of ones with an appropriate dimension. The mean packet service rate can be calculated by $\bar{\mu} = \varpi D_1 \mathbf{1}$, where ϖ is the steady state distribution of the absorbing Markov chain and can be calculated from $\varpi \mathbf{1} = 1$ and $\varpi D = \varpi$.

4.2 Energy Efficient Transmission Strategy

A sensor node can choose different transmission strategies based on the channel state, battery state and the number of buffered packets. Obviously, allocating more energy for data transmission in one slot can achieve better performance, i.e., a lower dropping packet probability and a smaller average delay, but it will accelerate the energy consumption as well. Motivated by threshold-based and state-aware scheduling strategies in [38, 50], the energy allocation has to be adaptively adjusted based on current system states. Intuitively, when a sensor node stores a large amount of packets in the buffer and holds sufficient energy for transmissions, in order to guarantee the system performance, more energy is allocated to achieve a higher successful transmission probability, i.e., a higher average service rate. In order to efficiently manage the energy allocation with QoS guarantees in terms of the reliability and timeliness, we propose a multi-threshold based transmission strategy to better balance the trade-off between the energy consumption and QoS performance provisioning.

In our proposed scheme, we define two threshold vectors $\boldsymbol{\nu}_E$ and $\boldsymbol{\nu}_D$ with $M + 1$ elements (i.e., thresholds) for partitioning the state spaces of data and energy queues, respectively. Without loss of generality, we assume $\phi_0 < \phi_1 < \dots < \phi_m < \dots < \phi_{M-1} < \phi_M, \phi_m \in \boldsymbol{\nu}_D$ and $\psi_0 < \psi_1 \leq \dots \leq \psi_m \leq \dots \leq \psi_{M-1} < \psi_M, \psi_m \in \boldsymbol{\nu}_E$, with $\phi_M = \ell_D, \psi_M = \ell_E$ representing full queues and $\phi_0 = \psi_0 = 0$ representing empty queues. Obviously, the threshold-based transmission strategy will divide the data queue

and energy queue into $M + 1$ successive intervals, $0, (\phi_0, \phi_1), [\phi_1, \phi_2), \dots, [\phi_{M-1}, \phi_M]$ and $0, (\psi_0, \psi_1), [\psi_1, \psi_2), \dots, [\psi_{M-1}, \psi_M]$. When data queue (energy queue) state is in the interval of $[\phi_{m-1}, \phi_m)$ ($[\psi_{m-1}, \psi_m)$), data queue (energy queue) is said to be at the m th stage.

According to the energy and data queue states, different energy units will be allocated. It is obvious that there are $(M + 1)^2$ combinations of energy and data stages based on our designed thresholds and the energy allocation for each combination should be specified. However, this may still result in high complexity and analysis difficulty. By considering the fact that current energy harvesting technologies are still at the early stage and the harvesting efficiency is still very low [71], we limit our focus on energy-saving transmission strategies. Specifically, with data queue at the m th stage and energy queue at the n th stage, θ_κ units of energy will be allocated for one packet transmission, where $\kappa = \min\{m, n\}$ and $\theta_\kappa \leq \psi_{n-1}$. Consequently, these $(M + 1)^2$ combinations are simplified into $M + 1$ cases. For instance, when the energy storage is low and data queue holds large amount of packets, we should allocate small amount of energy based on the energy queue state. On the contrary, when the amount of buffered packets is low and sensor has adequate energy storage, we still allocate small amount of energy based on the data queue state for the sake of reserving energy for future packet transmissions, since the average delay and packet dropping probability is already low when data queue length is small.

Therefore, $M + 1$ energy allocation levels $\Theta = \{\theta_\kappa, \kappa = 0, 1, 2, \dots, M\}$ will be constructed based on all the $M + 1$ cases. Considering efficient energy managements, we set $\theta_0 < \theta_1 \leq \dots \leq \theta_M$ with minimum energy consumption $\theta_0 = 0$. Since the packet service time is dependent on the channel condition and allocated energy, the service process in the κ th energy allocation level will follow the DMAP distribution with a pair representation $(D_0(\theta_\kappa), D_1(\theta_\kappa))$ with order K . The optimal threshold settings and energy allocations will be discussed in Chapter 4.4.

When $m = 0$, i.e., no packet exists in the system, we can derive the block matrices $B_{0,0}, B_{0,1}$ directly following a standard QBD.

$$B_{0,0} = \begin{bmatrix} \bar{\alpha}\bar{\beta} & \bar{\alpha}\beta & & & \\ & \bar{\alpha}\bar{\beta} & \bar{\alpha}\beta & & \\ & & \ddots & \ddots & \\ & & & \bar{\alpha}\bar{\beta} & \bar{\alpha}\beta \\ & & & & \bar{\alpha} \end{bmatrix} \otimes D(\theta_0), \quad (4.5)$$

$$B_{0,1} = \begin{bmatrix} \alpha\bar{\beta} & \alpha\beta & & & \\ & \alpha\bar{\beta} & \alpha\beta & & \\ & & \ddots & \ddots & \\ & & & \alpha\bar{\beta} & \alpha\beta \\ & & & & \alpha \end{bmatrix} \otimes D(\theta_0), \quad (4.6)$$

where the symbol \otimes denotes the Kronecker product. We take $B_{0,0}$ as an example to show the derivation process. $B_{0,0}$ denotes the case that there is no packet in the system and no new packet arrival at the end of the slot. Each row of $B_{0,0}$ represents the number of energy units in the system. Since $m = 0$, θ_0 is adopted for energy allocation, i.e. no energy is allocated. Since during the past time slot, the data queue remains empty and there is no energy consumption for data transmission, the corresponding probability with no energy arrival is $\bar{\alpha}\bar{\beta}D(\theta_0)$; otherwise, the probability is $\bar{\alpha}\beta D(\theta_0)$. When energy queue is full, since new energy arrivals will be dropped, the transition probability becomes $\bar{\alpha}D(\theta_0)$.

When $m \neq 0$, the transition sub-matrices will change from stage to stage. Here, we take the block matrix $B_{x,x-1}$ (when $x > 1$) as an example where a data packet is successfully transmitted. According to different energy queue status, $B_{x,x-1}$ consists of $M + 1$ subparts

$B_{1,0}, B_{1,1}, B_{1,2}$ which can be represented as

$$B_{1,0} = \begin{bmatrix} 0 \cdot I_K & 0 \cdot I_K & & & \\ \bar{\alpha}\bar{\beta}D_1(\theta_1) & \bar{\alpha}\beta D_1(\theta_1) & & & \\ & & \ddots & & \ddots \\ & & & & \bar{\alpha}\bar{\beta}D_1(\theta_1) & \bar{\alpha}\beta D_1(\theta_1) \end{bmatrix}, \quad (4.8)$$

$$B_{1,1} = \begin{bmatrix} \bar{\alpha}\bar{\beta} \cdot I_K & \bar{\alpha}\beta \cdot I_K & & & \\ \bar{\beta}\Gamma & \beta\Gamma & & & \\ & & \ddots & & \ddots \\ & & & & \bar{\beta}\Gamma & \beta\Gamma \end{bmatrix}, \quad (4.9)$$

$$B_{1,2} = \begin{bmatrix} \bar{\beta}\alpha \cdot I_K & \alpha\beta \cdot I_K & & & \\ \alpha\bar{\beta}D_0(\theta_1) & \alpha\beta D_0(\theta_1) & & & \\ & & \ddots & & \ddots \\ & & & & \alpha\bar{\beta}D_0(\theta_1) & \alpha\beta D_0(\theta_1) \end{bmatrix}, \quad (4.10)$$

where $\Gamma = (\bar{\alpha}D_0(\theta_1) + \alpha D_1(\theta_1))$, $\bar{\alpha} = 1 - \alpha$, $\bar{\beta} = 1 - \beta$, and I_K is the identity matrix with dimension of K .

After this level dependent QBD is constructed, a matrix analytic method can be used to obtain the stationary distribution. Let π be the stationary probability vector associated with the transition matrix \mathcal{P} . Vector π contains the steady state probabilities $\pi(x, y, c)$ corresponding to x data packets in the system, y units of energy in the battery, and channel state being c . Then π can be obtained from

$$\pi\mathcal{P} = \pi, \pi\mathbf{1} = 1, \quad (4.11)$$

where $\pi = [\pi_0, \pi_1, \dots, \pi_x, \dots, \pi_{\ell_D+1}]$, and each element π_x denotes the steady-state probability of x packets in the system. Based on matrix-geometric methods [72], we can

obtain the non-negative solutions R_x and G_x from

$$R_x = B_{x-1,x} + R_x B_{x,x} + R_x R_{x+1} B_{x+1,x}, \quad (4.12)$$

$$G_x = B_{x-1,x} + B_{x,x} G_x + B_{x+1,x} G_{x+1} G_x. \quad (4.13)$$

Given that this QBD process is positive recurrent, there exists a strictly positive solution to $\pi_0 = \pi_0(B_{0,0} + B_{0,1}G_1)$. And further we have the matrix product solution, $\pi_{x+1} = \pi_x R_x$.

4.3.2 Performance Measures

In this subsection, various performance measures are derived from the stationary distribution π .

Queue length distribution

Let $q_1(x)$ and $q_2(y)$ be the probabilities that there are x data packets in the system, and there are y units of energy in the system, respectively. Then, we have

$$q_1(x) = \sum_{y=0}^{\ell_E} \sum_{c=1}^K \pi(x, y, c), \quad \bar{q}_1 = \sum_x x q_1(x), \quad (4.14)$$

$$q_2(y) = \sum_{x=0}^{\ell_D+1} \sum_{c=1}^K \pi(x, y, c), \quad \bar{q}_2 = \sum_y y q_2(y), \quad (4.15)$$

where \bar{q}_1 and \bar{q}_2 represent corresponding average queue length.

Queueing throughput

A buffered data packet will be served eventually if it is not blocked upon its arrival. Thus, the queueing throughput is the mean number of transmitted packets within one slot, which can be calculated by

$$S = \alpha(1 - q_1(\ell_D + 1)). \quad (4.16)$$

Average energy waste

We define the energy units that were dropped due to a full energy queue as the energy waste, denoted by $\bar{\omega}$. Then, $\bar{\omega}$ (units/time slot) can be obtained from

$$\bar{\omega} = q_2(\ell_E)\beta. \quad (4.17)$$

Average delay

The average delay of buffered packets is the average time duration between a packet arrival and its departure. We can derive average delay $\bar{\tau}$ by using Little's Law as

$$\bar{\tau} = \frac{\bar{q}_1}{S}. \quad (4.18)$$

Average system-offline probability

We define the system is at offline state if the whole service is suspended when there is no energy available for data transmissions. Since the energy queue is empty at the offline state, the average system-offline probability $\bar{\delta}$ can be calculated by

$$\bar{\delta} = q_2(0). \quad (4.19)$$

4.4 Energy Efficiency Optimization

According to the analysis procedure shown in the previous section, it is important to set thresholds and corresponding energy allocations appropriately for specific application requirements. For explanation purpose, we focus on finding an optimal strategy such that energy efficiency is maximized subject to the constraints on the average delay and system-offline probability. Here, the energy efficiency is defined as the queueing throughput per

unit-energy consumption. Such optimization problem can be formulated as follows,

$$\begin{aligned}
& \max_{\nu_E, \nu_D, \Theta} \quad \frac{\mathcal{S}}{\bar{\beta}} & (4.20) \\
& \text{s.t.} \quad \bar{\tau} \leq \hat{\tau}, & (a) \\
& \quad \quad \bar{\delta} \leq \hat{\delta}, & (b) \\
& \quad \quad \phi_0 < \phi_1 < \cdots < \phi_M, & (c) \\
& \quad \quad \psi_0 < \psi_1 \leq \cdots \leq \psi_M, & (d) \\
& \quad \quad \theta_0 < \theta_1 \leq \cdots \leq \theta_M. & (e)
\end{aligned}$$

where ν_E, ν_D, Θ are decision variables. Constraints (a) and (b) aim to guarantee the requirements for the average delay and system-offline probability, respectively, where $\hat{\tau}$ and $\hat{\delta}$ are predefined. According to our previous discussions, thresholds settings for data queue and energy queue are constrained by (c) and (d), respectively, and the energy allocation levels are limited in constraint (e).

Note that transition probability matrices are functions of our decision variables, and close-form expressions for queue length distributions and performance metrics are commonly not available. However, by considering the fact that the number of thresholds, M , adopted by the sensor node in WBANs is usually not too large, we can adopt heuristic direct search techniques, such as the Hooke and Jeeves direct search method [65], to find the optimal strategy.

4.5 Numerical Results

A time-driven simulator is developed in Matlab to evaluate the system performance and validate the correctness of our analytical model. For each parameter setting, we conduct 10 simulations and the time length of each simulation is 10^6 slots. A Matlab toolbox in [73] and direct search method in [65] are used to solve the level dependent QBD chain and obtain the optimal strategy, respectively. We consider a Gilbert-Elliott correlated channel

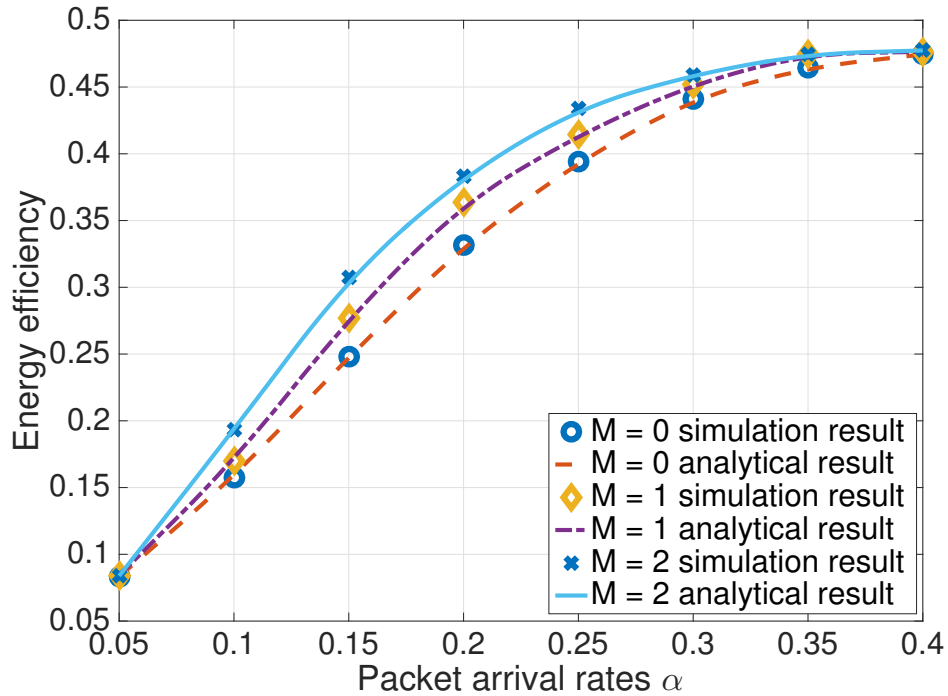


Figure 4.2: Energy efficiency comparison for different transmission strategies

with parameters $K = 2, P_{1,1} = 0.6, P_{1,2} = 0.4, P_{2,1} = 0.3, P_{2,2} = 0.7$, and buffer lengths are set to $\ell_D = 12, \ell_E = 12$. We investigate performance results for different transmission strategies (i.e., $M = 0, 1, 2$) with increasing data arrival rates.

In Figs. 4.2 - 4.5, we evaluate the system performance versus packet arrival rates for three different transmission strategies under a constant energy arrival rate $\beta = 0.4$. Obviously, all the simulation results match the analytical results very well, which justifies the accuracy of our proposed queueing analytical model. It can also be seen from the figures that multi-threshold ($M = 2$) transmission strategy outperforms the single-threshold ($M = 1$) and non-threshold ($M = 0$) strategies in terms of average energy waste, average delay and packet dropping probability. It is because our threshold-based transmission strategies can efficiently utilize the harvested energy by allowing more flexible energy allocations based on system states.

In addition, as we expected, when the arrival rate increases, the packet dropping probability, average delay and energy efficiency increase for all strategies due to high

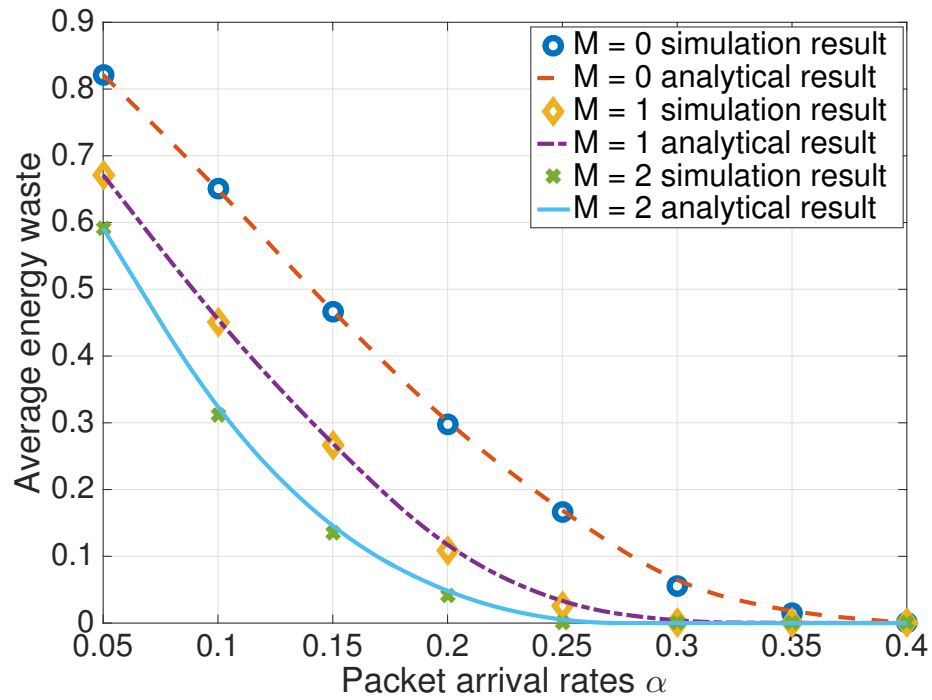


Figure 4.3: Energy waste comparison for different transmission strategies

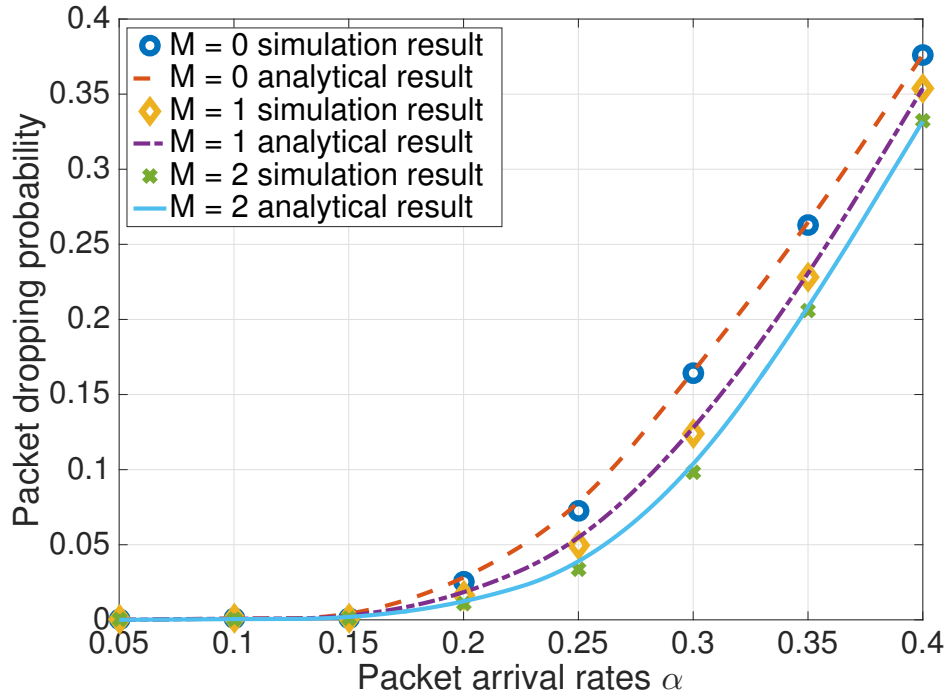


Figure 4.4: Packet dropping probability comparison for different transmission strategies

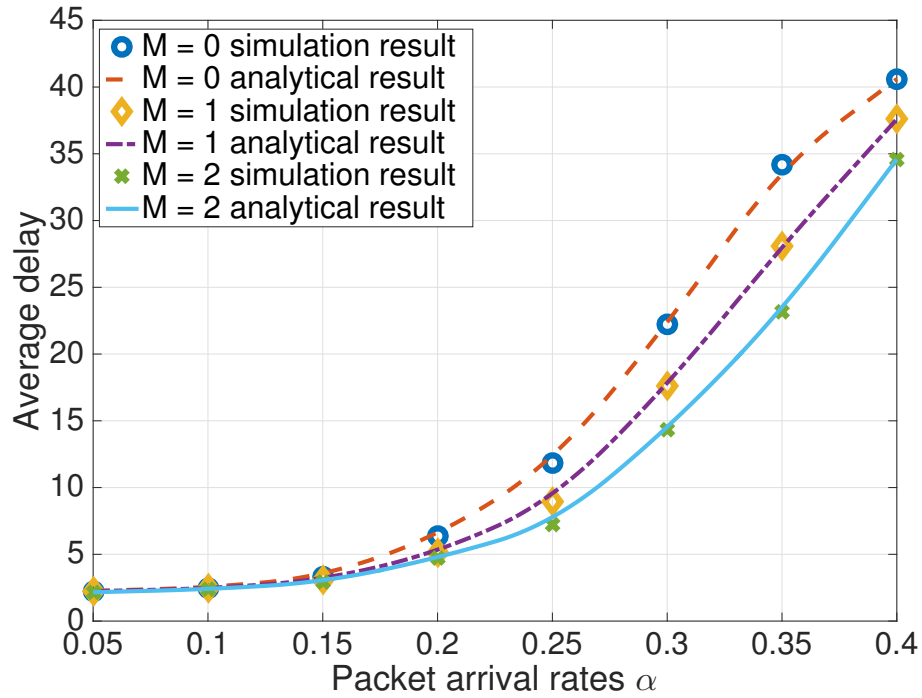


Figure 4.5: Average delay comparison for different transmission strategies

arrival traffics while the average energy waste decreases. Note that when a very high data arrival rate is applied, the energy waste for all strategies is close to zero, and poor QoS performance such as long average waiting time and high dropping probability become inevitable. This is because the energy storage becomes insufficient with large amounts of data packets waiting for transmissions. Consequently, the performance gap between non-threshold and threshold-based strategies is relatively small at this case. Moreover, we can also observe that when the packet arrival rate is low, the packet dropping probability and the average delay gradually approach zeros for all strategies, but the non-threshold strategy waste much more energy than threshold-based ones. Except those two extreme cases, the superiority of threshold-based strategies is obvious. It can also be expected that the transmission strategy with more thresholds is more flexible in energy allocation and can better adapt to the dynamics of system states.

Chapter 5

Conclusions and Future Works

5.1 Conclusion and Comments

In this thesis, the network characteristics, communication architecture, and potential applications of WBANs have been firstly reviewed. Then the new research challenges resulting from the complicated channel environments and more stringent energy efficient requirements in WBANs were illustrated in Chapter 2. Since our research mainly focuses on the packet transmission scheduling in WBANs, a comprehensive literature survey on recent scheduling designs were also provided.

In Chapter 3, a queueing analytical framework has been presented to analyze the performances of a WBAN with instantaneous delay constraints and human body shadowing effects. Through carefully analyzing the MAC mechanism defined in the IEEE 802.15.6, we developed a PH distribution with a specific blocking rate to model the access process. A random time limited vacation has been considered to describe the random shadowing interruption process, i.e., random blocking and random recovering of the service. In addition, a buffer length optimization problem has been solved to approximately model the effects of instantaneous delay constraints. To make the proposed analytical framework more general and comprehensive, we introduced the MAP distribution for modeling arrival traffics and PH distributions to mathematically describe the service process and

random interruption vacation. Theoretical and simulation results showed that the proposed analytical framework was both accurate and computationally efficient. In addition, the results also demonstrated that instantaneous delay constraints could guarantee the timeliness of served packets and the human body shadowing had considerable effects on the packet average delay and transmission failure probability.

In Chapter 4, we have presented a multi-threshold based packet transmission strategy for a rechargeable sensor in WBANs. Sensors can efficiently allocate the transmission energy while jointly taking into account the battery state and data buffer state. A general discrete-time queueing system is constructed for performance evaluations of our proposed scheme. After deriving various performance metrics through analyzing a level dependent QBD Markov chain, an optimization problem is formulated to investigate optimal threshold configurations for maximizing the energy efficiency with QoS guarantee. Numerical results verify our analytical models and demonstrate performance gains of our proposed strategy.

5.2 Future Works

In our proposed multi-threshold based packet transmission strategies, we considered a simple channel model without modeling the human body shadowing effects, and assumed the geometric distributions for both data and energy arrivals. A more practical extension is to consider the shadowing interruptions and adopt more practical distributions to capture the arrival correlations. Besides, to achieve a better energy efficiency, we can also apply the instantaneous delay constraints like we proposed in Chapter 3 into the joint data and energy scheduling issues. However, these extensions will cause great analyses difficulties, which require more advanced queueing theory and more reasonable approximation methods. In addition, since the sensor cannot transmit data and collect energy simultaneously in some practical scenarios, studying the optimal pattern selection policy for the sensor also becomes necessary.

In our presented analytical framework, the human body shadowing could randomly

interrupt the packet transmission, i.e., the service rate becomes zero when the server starts a shadowing vacation. One potential extension is to consider the service degradation when shadowing vacation occurs instead of complete interruptions. Moreover, a priority queueing structure may also be taken into account to introduce the effects of the emergency traffics. Apart from the instantaneous delay constraints, we may also consider a priority-changing scheme to improve the emergency data transmissions. For example, we can consider the priority falling scheme between different class priority queues based on the packet waiting time [43]. Moreover, for future works, extensive real experiments need to be carried out to verify our analysis and test the performance of our proposed multi-threshold transmission strategies.

In addition, my current research mainly focuses on intra-WBANs, where the interference among multiple WBANs (inter-WBANs) has not been considered. However, the data transmission of WBANs in practice may be influenced by the interfering neighbors. Specifically, human motions that are commonly highly unpredictable may result in the WBAN randomly moving into and out of each other's coverage, which will cause severe mutual interference. Obviously, the existence of the unexpected interference will inevitably cause grate performance degradation on our proposed transmission scheduling schemes. Thus not only the energy efficiency and channel randomness but also the inter-WBAN interference mitigation should be carefully considered. Therefore, exploring a robust transmission scheduling design to support multiple WBANs scenarios without compromising QoS requirements will be another interesting future work.

Reference

- [1] S. Movassaghi, M. Abolhasan, J. Lipman, D. Smith, and A. Jamalipour, “Wireless body area networks: A survey,” *IEEE Communications Surveys & Tutorials*, vol. 16, no. 3, pp. 1658–1686, 2014.
- [2] M. Patel and J. Wang, “Applications, challenges, and prospective in emerging body area networking technologies,” *IEEE Wireless communications*, vol. 17, no. 1, 2010.
- [3] L. Hanlen, D. Smith, A. Boulis, B. Gilbert, V. Chaganti, L. Craven, D. Fang, T. Lamahewa, D. Lewis, D. Miniutti, O. Nagy, D. Rodda, K. Sithamparanathan, Y. Tselishchev, and A. Zhang, “Wireless body area networks : toward a wearable intranet,” in *National ICT Australia*, 2011.
- [4] R. Cavallari, F. Martelli, R. Rosini, C. Buratti, and R. Verdone, “A survey on wireless body area networks: Technologies and design challenges,” *IEEE Communications Surveys & Tutorials*, vol. 16, no. 3, pp. 1635–1657, 2014.
- [5] M. A. Hanson, H. C. Powell Jr, A. T. Barth, K. Ringgenberg, B. H. Calhoun, J. H. Aylor, and J. Lach, “Body area sensor networks: Challenges and opportunities,” *Computer*, vol. 42, no. 1, p. 58, 2009.
- [6] A. Argyriou, A. C. Breva, and M. Aoun, “Optimizing data forwarding from body area networks in the presence of body shadowing with dual wireless technology nodes,” *IEEE Transactions on Mobile Computing*, vol. 14, no. 3, pp. 632–645, 2015.
- [7] E. Reusens, W. Joseph, G. Vermeeren, L. Martens, B. Latré, I. Moerman, B. Braem, and C. Blondia, “Path loss models for wireless communication channel along arm and torso: measurements and simulations,” in *Antennas and Propagation Society International Symposium, 2007 IEEE*. IEEE, 2007, pp. 345–348.
- [8] Y. I. Nechayev, P. S. Hall, C. C. Constantinou, Y. Hao, A. Alomainy, R. Dubrovka, and C. G. Parini, “On-body path gain variations with changing body posture and antenna position,” in *Antennas and Propagation Society International Symposium, 2005 IEEE*, vol. 1. IEEE, 2005, pp. 731–734.
- [9] T. Camp, J. Boleng, and V. Davies, “A survey of mobility models for ad hoc network research,” *Wireless communications and mobile computing*, vol. 2, no. 5, pp. 483–502, 2002.
- [10] D. Niyato, E. Hossain, and A. Fallahi, “Sleep and wakeup strategies in solar-powered wireless sensor/mesh networks: Performance analysis and optimization,” *IEEE Transactions on Mobile Computing*, vol. 6, no. 2, 2007.

- [11] K. Akkaya and M. Younis, "A survey on routing protocols for wireless sensor networks," *Ad hoc networks*, vol. 3, no. 3, pp. 325–349, 2005.
- [12] J. Luprano, J. Solà, S. Dasen, J. M. Koller, and O. Chételat, "Combination of body sensor networks and on-body signal processing algorithms: the practical case of myheart project," in *Wearable and Implantable Body Sensor Networks, 2006. BSN 2006. International Workshop on*. IEEE, 2006, pp. 4–pp.
- [13] H. Li and J. Tan, "Heartbeat-driven medium-access control for body sensor networks," *IEEE Transactions on Information Technology in Biomedicine*, vol. 14, no. 1, pp. 44–51, 2010.
- [14] K. Christensen, G. Doblhammer, R. Rau, and J. W. Vaupel, "Ageing populations: the challenges ahead," *The lancet*, vol. 374, no. 9696, pp. 1196–1208, 2009.
- [15] Q. Shen, X. Liang, X. Shen, X. Lin, and H. Y. Luo, "Exploiting geo-distributed clouds for a e-health monitoring system with minimum service delay and privacy preservation," *IEEE Journal of Biomedical and Health Informatics*, vol. 18, no. 2, pp. 430–439, 2014.
- [16] X. Xu, L. Shu, and et. al., "A survey on energy harvesting and integrated data sharing in wbans," *International Journal of Distributed Sensor Networks*, vol. 2015, no. 1, 2015.
- [17] S. N. Ramli and R. Ahmad, "Surveying the wireless body area network in the realm of wireless communication," in *Information Assurance and Security (IAS), 2011 7th International Conference on*. IEEE, 2011, pp. 58–61.
- [18] B. Latré, B. Braem, I. Moerman, C. Blondia, and P. Demeester, "A survey on wireless body area networks," *Wireless Networks*, vol. 17, no. 1, pp. 1–18, 2011.
- [19] B. Gyselinckx, R. Vullers, C. Van Hoof, J. Ryckaert, R. F. Yazicioglu, P. Fiorini, and V. Leonov, "Human++: Emerging technology for body area networks," in *Very large scale integration, 2006 IFIP international conference on*. IEEE, 2006, pp. 175–180.
- [20] o. N.-I. R. H. IEEE Standards Coordinating Committee 28, *IEEE Standard for Safety Levels with Respect to Human Exposure to Radio Frequency Electromagnetic Fields, 3kHz to 300 GHz*. Institute of Electrical and Electronics Engineers, Incorporated, 1992.
- [21] H. Cao, V. Leung, C. Chow, and H. Chan, "Enabling technologies for wireless body area networks: A survey and outlook," *IEEE Communications Magazine*, vol. 47, no. 12, 2009.
- [22] S. Ullah, H. Higgins, B. Braem, B. Latre, C. Blondia, I. Moerman, S. Saleem, Z. Rahman, and K. S. Kwak, "A comprehensive survey of wireless body area networks," *Journal of medical systems*, vol. 36, no. 3, pp. 1065–1094, 2012.
- [23] M. Chen, S. Gonzalez, A. Vasilakos, H. Cao, and V. C. Leung, "Body area networks: A survey," *Mobile networks and applications*, vol. 16, no. 2, pp. 171–193, 2011.
- [24] "Ieee standard for local and metropolitan area networks - part 15.6: Wireless body area networks," *IEEE Std 802.15.6-2012*, Feb 2012.
- [25] C. Otto, A. Milenkovic, C. Sanders, and E. Jovanov, "System architecture of a wireless body area sensor network for ubiquitous health monitoring," *Journal of mobile multimedia*, vol. 1, no. 4, pp. 307–326, 2006.

- [26] K. S. Kwak, S. Ullah, and N. Ullah, "An overview of ieee 802.15. 6 standard," in *Applied Sciences in Biomedical and Communication Technologies (ISABEL), 2010 3rd International Symposium on*. IEEE, 2010, pp. 1–6.
- [27] A. Boulis, D. Smith, D. Miniutti, L. Libman, and Y. Tselishchev, "Challenges in body area networks for healthcare: The mac," *IEEE Communications Magazine*, vol. 50, no. 5, 2012.
- [28] V. Tarokh, *New directions in wireless communications research*. Springer, 2009.
- [29] M. N. Deylami and E. Jovanov, "A distributed scheme to manage the dynamic coexistence of ieee 802.15. 4-based health-monitoring wbans," *IEEE journal of biomedical and health informatics*, vol. 18, no. 1, pp. 327–334, 2014.
- [30] B. de Silva, A. Natarajan, and M. Motani, "Inter-user interference in body sensor networks: Preliminary investigation and an infrastructure-based solution," in *Wearable and Implantable Body Sensor Networks, 2009. BSN 2009. Sixth International Workshop on*. IEEE, 2009, pp. 35–40.
- [31] J. Espina, H. Baldus, T. Falck, O. Garcia, and K. Klabunde, "Towards easy-to-use, safe, and secure wireless medical body sensor networks," in *Mobile Health Solutions for Biomedical Applications*. IGI Global, 2009, pp. 159–179.
- [32] L. Wang and Y. Xiao, "A survey of energy-efficient scheduling mechanisms in sensor networks," *Mobile Networks and Applications*, vol. 11, no. 5, pp. 723–740, 2006.
- [33] S. A. Gopalan and J.-T. Park, "Energy-efficient mac protocols for wireless body area networks: survey," in *Ultra Modern Telecommunications and Control Systems and Workshops (ICUMT), 2010 International Congress on*. IEEE, 2010, pp. 739–744.
- [34] A. Boulis, D. Smith, D. Miniutti, L. Libman, and Y. Tselishchev, "Challenges in body area networks for healthcare: the mac," *IEEE Communications Magazine*, vol. 50, no. 5, pp. 100–106, May 2012.
- [35] O. Omeni, A. C. W. Wong, A. J. Burdett, and C. Toumazou, "Energy efficient medium access protocol for wireless medical body area sensor networks," *IEEE Transactions on biomedical circuits and systems*, vol. 2, no. 4, pp. 251–259, 2008.
- [36] S. J. Marinkovic, E. M. Popovici, C. Spagnol, S. Faul, and W. P. Marnane, "Energy-efficient low duty cycle mac protocol for wireless body area networks," *IEEE Transactions on Information Technology in Biomedicine*, vol. 13, no. 6, pp. 915–925, 2009.
- [37] T. O'Donovan, J. O'Donoghue, C. Sreenan, D. Sammon, P. O'Reilly, and K. A. O'Connor, "A context aware wireless body area network (ban)," in *Pervasive Computing Technologies for Healthcare, 2009. PervasiveHealth 2009. 3rd International Conference on*. IEEE, 2009, pp. 1–8.
- [38] H. Su and X. Zhang, "Battery-dynamics driven tdma mac protocols for wireless body-area monitoring networks in healthcare applications," *IEEE Journal on selected areas in communications*, vol. 27, no. 4, 2009.
- [39] J. Abate, G. L. Choudhury, and W. Whitt, "Waiting-time tail probabilities in queues with long-tail service-time distributions," *Queueing systems*, vol. 16, no. 3, pp. 311–338, 1994.

- [40] S. De Vuyst, S. Wittevrongel, and H. Bruneel, "Mean value and tail distribution of the message delay in statistical multiplexers with correlated train arrivals," *Performance Evaluation*, vol. 48, no. 1, pp. 103–129, 2002.
- [41] H. Ghasemzadeh, V. Loseu, S. Ostadabbas, and R. Jafari, "Burst communication by means of buffer allocation in body sensor networks: Exploiting signal processing to reduce the number of transmissions," *IEEE Journal on Selected Areas in Communications*, vol. 28, no. 7, 2010.
- [42] V. Raghunathan, C. Schurgers, S. Park, and M. B. Srivastava, "Energy-aware wireless microsensor networks," *IEEE Signal processing magazine*, vol. 19, no. 2, pp. 40–50, 2002.
- [43] Z. Zhao, C. Yi, J. Cai, and H. Cao, "Queueing analysis for medical data transmissions with delay-dependent packet priorities in wbans," in *2016 8th International Conference on Wireless Communications Signal Processing (WCSP)*, Oct 2016, pp. 1–5.
- [44] S. Ulukus, A. Yener, E. Erkip, O. Simeone, M. Zorzi, P. Grover, and K. Huang, "Energy harvesting wireless communications: A review of recent advances," *IEEE Journal on Selected Areas in Communications*, vol. 33, no. 3, pp. 360–381, 2015.
- [45] "Ieee standard for local and metropolitan area networks - part 15.6: Wireless body area networks," *IEEE Std 802.15.6-2012*, Feb 2012.
- [46] M. L. Puterman, *Markov decision processes: discrete stochastic dynamic programming*. John Wiley & Sons, 2014.
- [47] A. Seyedi and B. Sikdar, "Energy efficient transmission strategies for body sensor networks with energy harvesting," *IEEE Trans. Commun.*, vol. 58, no. 7, pp. 2116–2126, 2010.
- [48] D. Niyato, P. Wang, Y. W. Leong, and T. H. Pink, "Qos-aware data transmission and wireless energy transfer: Performance modeling and optimization," in *WCNC*. IEEE, 2014, pp. 3100–3105.
- [49] S. Xiao, A. Dhamdhere, V. Sivaraman, and A. Burdett, "Transmission power control in body area sensor networks for healthcare monitoring," *IEEE J. Sel. Areas Commun.*, vol. 27, no. 1, pp. 37–48, 2009.
- [50] F. Chiti, R. Fantacci, F. Archetti, E. Messina, and D. Toscani, "An integrated communications framework for context aware continuous monitoring with body sensor networks," *IEEE J. Sel. Areas Commun.*, vol. 27, no. 4, 2009.
- [51] S. Movassaghi, M. Abolhasan, J. Lipman, D. Smith, and A. Jamalipour, "Wireless body area networks: A survey," *IEEE Commun. Surveys Tuts.*, vol. 16, no. 3, pp. 1658–1686, 2014.
- [52] P. Ferrand, J.-M. Gorce, and C. Goursaud, "On the packet error rate of correlated shadowing links in ban," in *Proceedings of the 5th European Conference on Antennas and Propagation*. IEEE, 2011, pp. 3094–3098.
- [53] S. Rashwand and J. Mistic, "Performance evaluation of ieee 802.15. 6 under non-saturation condition," in *Global Telecommunications Conference (GLOBECOM 2011), 2011 IEEE*. IEEE, 2011, pp. 1–6.

- [54] S. Rashwand, J. Mišić, and H. Khazaei, “Performance analysis of ieee 802.15. 6 under saturation condition and error-prone channel,” in *Wireless Communications and Networking Conference (WCNC), 2011 IEEE*. IEEE, 2011, pp. 1167–1172.
- [55] S. Ullah, M. Chen, and K. S. Kwak, “Throughput and delay analysis of ieee 802.15. 6-based csma/ca protocol,” *Journal of medical systems*, vol. 36, no. 6, pp. 3875–3891, 2012.
- [56] S. Sarkar, S. Misra, B. Bandyopadhyay, C. Chakraborty, and M. S. Obaidat, “Performance analysis of ieee 802.15. 6 mac protocol under non-ideal channel conditions and saturated traffic regime,” *IEEE Transactions on computers*, vol. 64, no. 10, pp. 2912–2925, 2015.
- [57] J. J. Hunter, *Mathematical Techniques of Applied Probability: Discrete Time Models: Basic Theory*. Academic Press, 2014, vol. 1.
- [58] A. Taparugssanagorn, A. Rabbachin, M. Hämäläinen, J. Saloranta, J. Iinatti *et al.*, “A review of channel modelling for wireless body area network in wireless medical communications,” 2008.
- [59] I. Khan, Y. I. Nechayev, and P. S. Hall, “On-body diversity channel characterization,” *IEEE Transactions on Antennas and Propagation*, vol. 58, no. 2, pp. 573–580, 2010.
- [60] T. S. Rappaport *et al.*, *Wireless communications: principles and practice*. Prentice Hall PTR New Jersey, 1996, vol. 2.
- [61] J. Wang, A. Huang, L. Cai, and W. Wang, “On the queue dynamics of multiuser multichannel cognitive radio networks,” *IEEE Transactions on Vehicular Technology*, vol. 62, no. 3, pp. 1314–1328, 2013.
- [62] A. S. Alfa, *Queueing theory for telecommunications: discrete time modelling of a single node system*. Springer, 2010.
- [63] M. A. Johnson and M. R. Taaffe, “Matching moments to phase distributions: Mixtures of erlang distributions of common order,” *Stochastic Models*, vol. 5, no. 4, pp. 711–743, 1989.
- [64] B. Doytchinov, J. Lehoczy, and S. Shreve, “Real-time queues in heavy traffic with earliest-deadline-first queue discipline,” *Annals of Applied Probability*, vol. 11, no. 2, pp. 332–378, 2001.
- [65] R. Hooke and T. A. Jeeves, ““direct search” solution of numerical and statistical problems,” *Journal of the ACM (JACM)*, vol. 8, no. 2, pp. 212–229, 1961.
- [66] N. Akar, N. C. Oğuz, and K. Sohraby, “A novel computational method for solving finite qbd processes,” *Stochastic Models*, vol. 16, no. 2, pp. 273–311, 2000.
- [67] A. Fallahi and E. Hossain, “Distributed and energy-aware mac for differentiated services wireless packet networks: a general queuing analytical framework,” *IEEE Transactions on Mobile Computing*, vol. 6, no. 4, 2007.
- [68] D. Bini, B. Meini, S. Steffé, and B. Van Houdt, “Structured markov chains solver: software tools,” in *Proceeding from the 2006 workshop on Tools for solving structured Markov chains*. ACM, 2006, p. 14.

- [69] A. Dudin, M. H. Lee, and S. Dudin, "Optimization of the service strategy in a queueing system with energy harvesting and customers impatience," *International Journal of Applied Mathematics and Computer Science*, vol. 26, no. 2, pp. 367–378, 2016.
- [70] Q. Zhang and S. A. Kassam, "Finite-state markov model for rayleigh fading channels," *IEEE Trans. Commun.*, vol. 47, no. 11, pp. 1688–1692, Nov 1999.
- [71] Y. He, X. Cheng, W. Peng, and G. L. Stuber, "A survey of energy harvesting communications: models and offline optimal policies," *IEEE Communications Magazine*, vol. 53, no. 6, pp. 79–85, 2015.
- [72] A. S. Alfa, *Applied discrete-time queues*. Springer, 2015.
- [73] T. Dayar and M. C. Orhan, "Kronecker-based infinite level-dependent qbd processes," *Journal of Applied Probability*, vol. 49, no. 04, pp. 1166–1187, 2012.

Publication List

- [J1] **Z. Zhao**, S. Huang, and J. Cai, "An analytical framework for IEEE 802.15.6-based wireless body sensor networks with instantaneous delay constraints and shadowing interruptions," submitted to *IEEE Transactions on Vehicular Technology*.
- [J2] C. Yi, **Z. Zhao**, J. Cai, R.L. Faria, and G. Zhang, "Priority-aware pricing-based capacity sharing scheme for beyond-wireless body area networks," *Computer Networks*, vol. 98, pp. 29-43, Apr. 2016.
- [C1] **Z. Zhao**, S. Huang, and J. Cai, "Energy efficient packet transmission strategies for wireless body area networks with rechargeable sensors," (**Invited Paper**) *IEEE Vehicular Technology Conference (VTC'2017-Fall)*.
- [C2] **Z. Zhao**, C. Yi, J. Cai, and H. Cao, "Queueing analysis for medical packet transmission with delay-dependent packet priorities in WBANs," *IEEE Conference on Wireless Communications and Signal Processing (WCSP'2016)*, Jiangsu, China, Oct. 13-15, 2016.
- [C3] H. Cao, J. Cai, A. S. Alfa, and **Z. Zhao**, "Efficient resource allocation scheduling for MIMO-OFDMA-CR downlink systems," *IEEE Conference on Wireless Communications and Signal Processing (WCSP'2016)*, Jiangsu, China, Oct. 13-15, 2016.